Earthquake Early Warning

S. Parolai

Seismic Risk Assessment and Mitigation

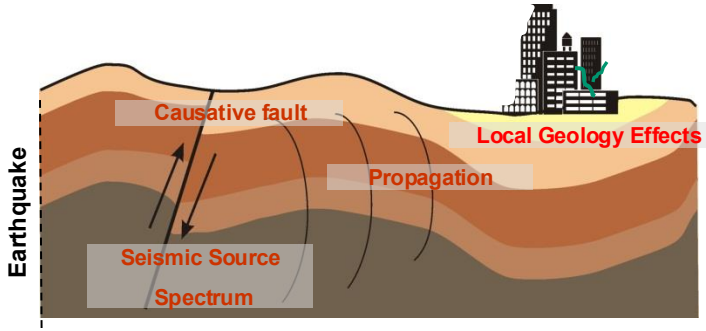

Decades | Years | Days to minutes | 0 | seconds | Minutes to hours

Long Term Seismic and landslides Risk mapping

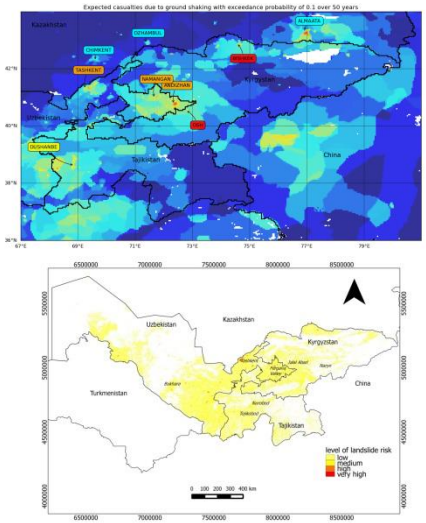

Long Term Forecasting

Short Term Forecasting

Earthquake and landslides Early Warning

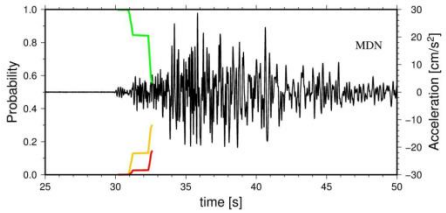

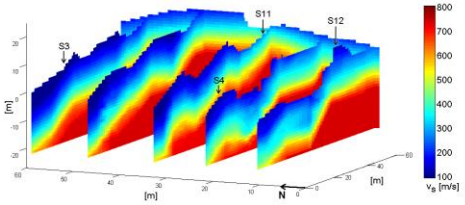

Real time and rapid loss estimation

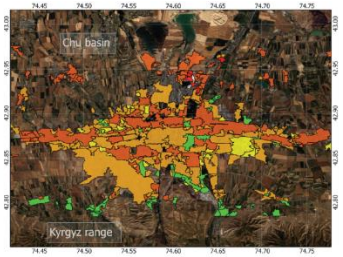

Aftershock Forecasting

Objective

The goal of an EEW system is the estimation in a fast and reliable way an earthquake's damage potential before the strong shaking hits the target

Principles

The idea of developing systems for launching early alert messages about incoming ground shaking dates back to 1868 (*Cooper JD, Letter to the Editor, San Francisco Daily Evening Bulletin, November 3, 1868*). It is based on the fact that information spread through electromagnetic signals travels faster (about 300,000 km/s) than seismic waves (a few km/s). Moreover, most of the radiated seismic energy is carried by S- and surface-waves, which travel slower than P-waves.

Early examples

The first early warning systems were developed and installed during the cold war to detect incoming intercontinental ballistic missiles. These early warning systems were designed to alert target areas as soon as a missile was detected by a radar or a launch discovered by satellite systems.

from
Satriano et al., SDEE, 2011

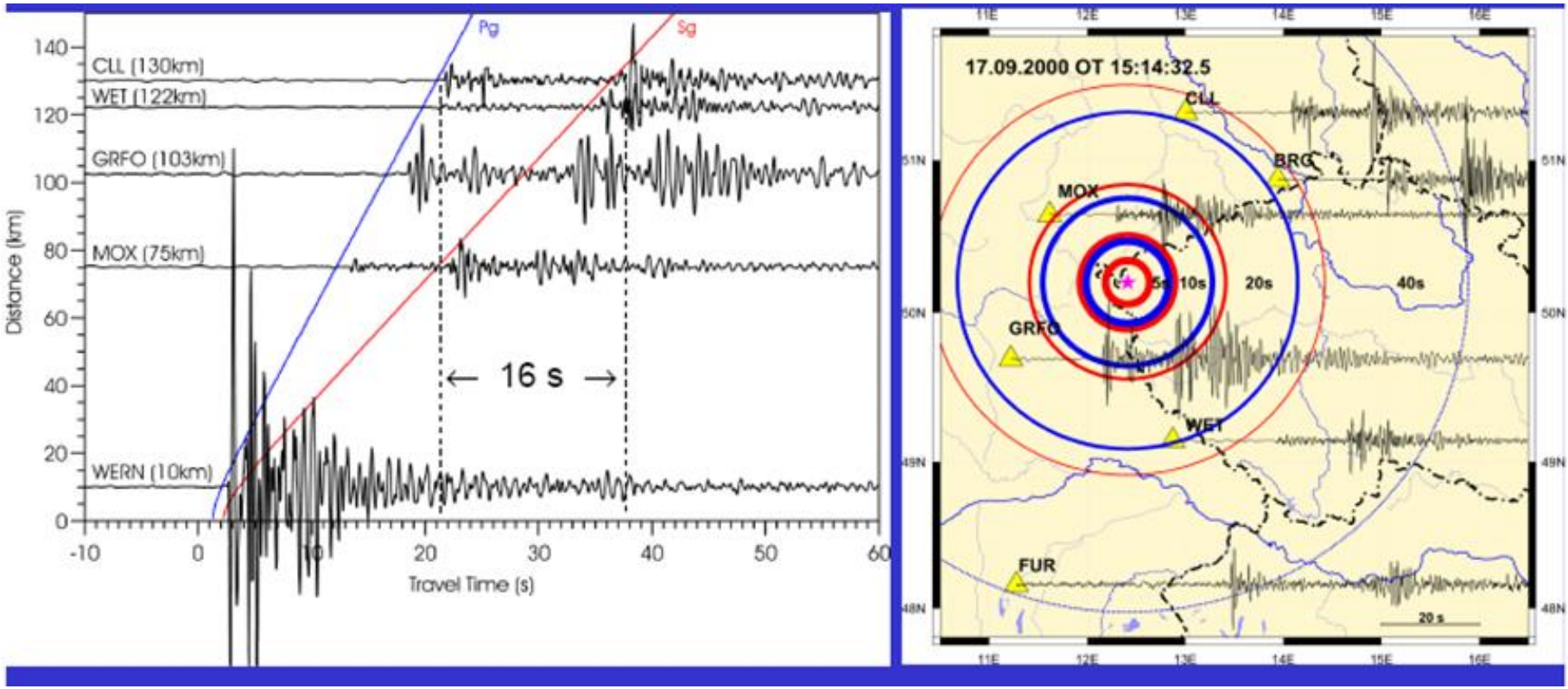
Pg
Sg
CLL (130km)
WET (122km)
GRFO (103km)
MOX (75km)
WERN (10km)
← 16 s →
Distance (km)
Travel Time (s)
17.09.2000 OT 15:14:32.5
CLL
BRG
MOX
GRFO
WET
FUR
5s
10s
20s
40s
20 s

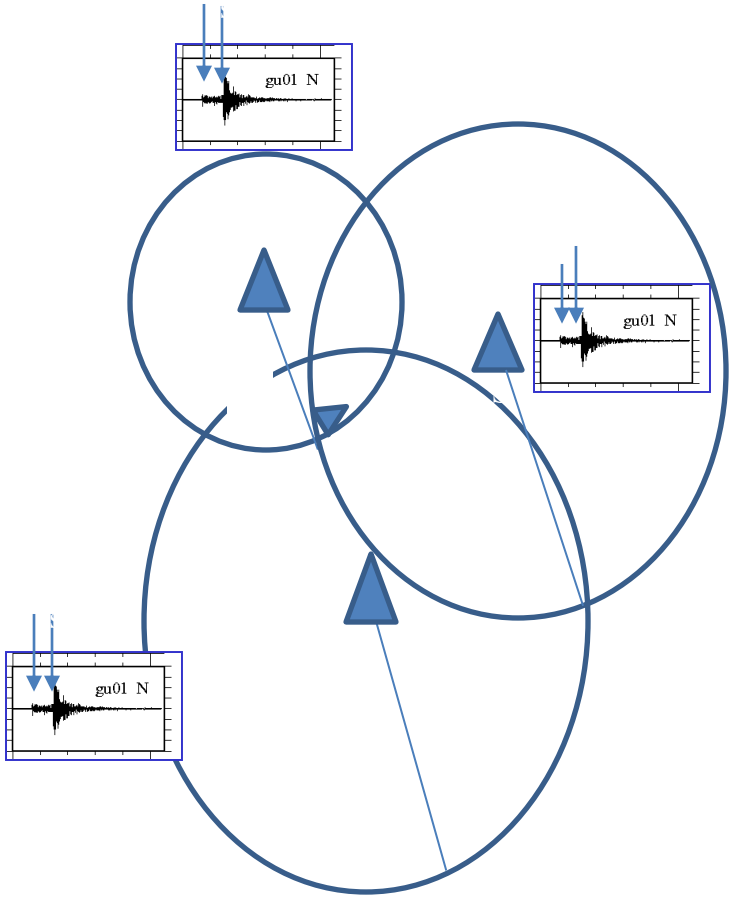
gu01 N
gu01 N
gu01 N

Confronto tra diversi metodi per la localizzazione dei terremoti

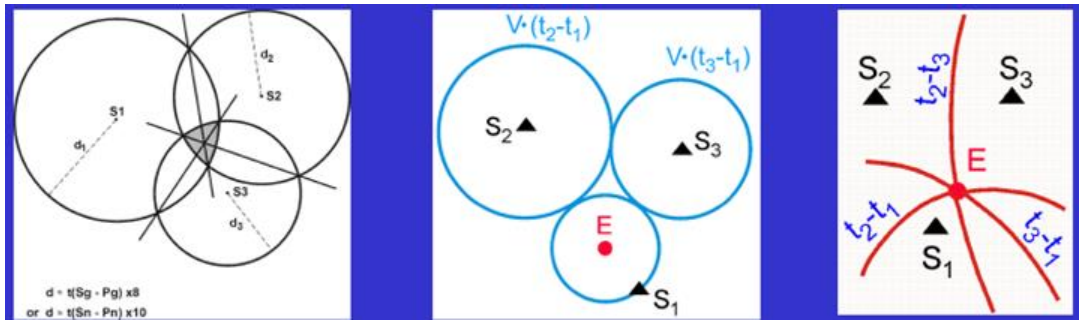

Tutti i metodi illustrati non considerano la forma della terra, e si basano su distanze planari cioè possono essere applicati solo su piccola scala, a livello locale.
Allo stesso modo, tutti i metodi si basano sul modello calcolo dei tempi di percorso mostrato nella diapositiva precedente

Geigers Method

Given a set of M arrival times t_i find the origin time t_0 and the hypocentre in cartesian coordinatios (x_0, y_0, z_0) which minimize the objective function

$$F(\mathbf{X}) = \sum_{i=1}^{M} r_i^2.$$

Here, r_i is the difference between observed and calculated arrival times

$$r_i = t_i - t_0 - T_i,$$

and the unknown parameter vector is

$$\mathbf{X} = (t_0, x_0, y_0, z_0)^{\mathrm{T}}$$

In matrix form (1) becomes

$$F(\mathbf{X}) = \mathbf{r}^{\mathrm{T}}\mathbf{r}$$

Geigers Method

The Gauss--Newton procedure requires an initial guess of the sought parameters, denoted here as

$$\mathbf{X}^* = (t_0^*, x_0^*, y_0^*, z_0^*)^{\mathbf{T}},$$

which are then used to calculate the adjustment vector

$$\delta\mathbf{X} = (\delta t_0, \delta x_0, \delta y_0, \delta z_0)^{\mathrm{T}}$$

in

$$(1)\mathbf{A}^{\mathrm{T}}\mathbf{A}\delta\mathbf{X} = -\mathbf{A}^{\mathrm{T}}\mathbf{r}.$$

The Jacobian matrix $\mathbf{A}$ is defined as

$$\mathbf{A} = \begin{pmatrix} \partial r_1/\partial t_0 & \partial r_1/\partial x_0 & \partial r_1/\partial y_0 & \partial r_1/\partial z_0 \\ \partial r_2/\partial t_0 & \partial r_2/\partial x_0 & \partial r_2/\partial y_0 & \partial r_2/\partial z_0 \\ \vdots & \vdots & \vdots & \vdots \\ \partial r_M/\partial t_0 & \partial r_M/\partial x_0 & \partial r_M/\partial y_0 & \partial r_M/\partial z_0 \end{pmatrix}.$$

The partial derivatives are evaluated at the initial guess, or trial vector, $\mathbf{X}^*$. Equation (45) can be rewritten as

$$(2)\mathbf{G}\delta\mathbf{X} = \mathbf{g}.$$

Using an initial guess of **X*** an adjustment vector can be calculated. The initial guess can then be updated **X*+δX** and used as the initial guess in the next run. In this way the sought parameters **X** can be determined with some tolerance

Approaches

There are two main approaches: **Regional** (or network-based) EEW systems and **Onsite** (or single-station) EEW systems.

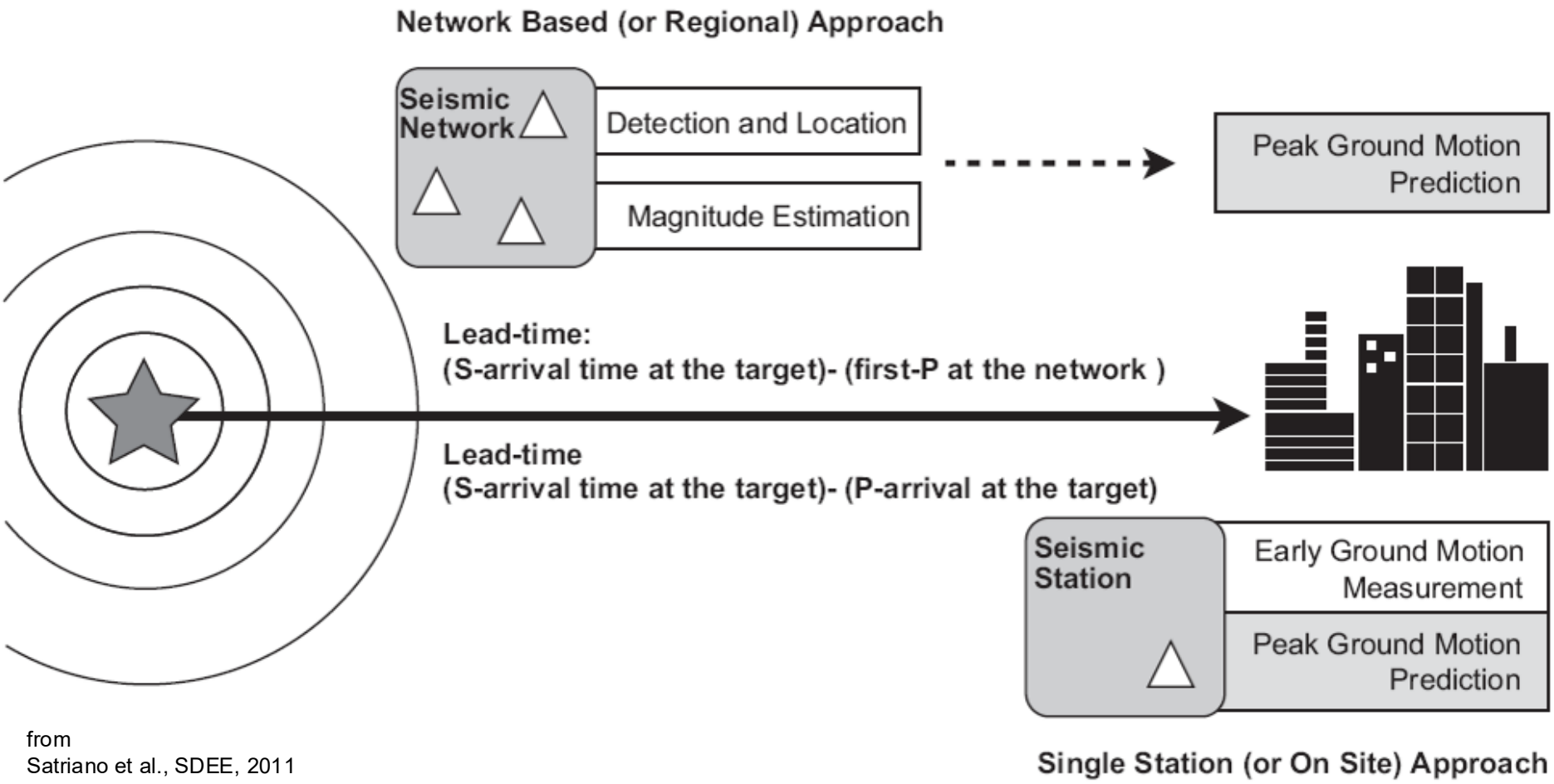

from
Satriano et al., SDEE, 2011

Methodology

Regional network EEW system

Event detection and location

Magnitude estimation

Peak ground motion prediction at target site

Alert notification

Onsite approaches predict the ground shaking associated with S-wave starting from the ground shaking recorded for P-waves.
Some Onsite (or single station) EEW systems also estimate the location and magnitude of the event (e.g., Nakamura approach; Odaka approach; etc).

Starting from the Regional and Onsite schemes, more complex and hybrid systems can be established. For example, Onsite systems can be composed of several nodes communicating witheach others and fed with information coming from a Regional networks. The Regional scheme may in turn simplified into a concept involving a front-detection scheme when the source region is known.

Time is a critical parameter in any EEW system. The system and procedures have to be designed in such a way as to maximize the **lead time** for the target area.

	Regional	**Onsite**
Network deployment	Source region	Target area
Data analysis	Network based	Single station
Output parameters	Location, magnitude	Location, magnitude or expected intensity
Accuracy on source parameter estimation	Good to high	Moderate
Lead-time	Ts at the target–Tp at the source	Ts at the target–Tp at the target

from
Satriano et al., SDEE, 2011

Lead time maximization and improvements in the estimation of parameters (such as magnitude, location) however involve a trade-off. The minimization of the false alarms is also crucial.

Therefore, any EEW system has to be tailored to the specific situation at hand.

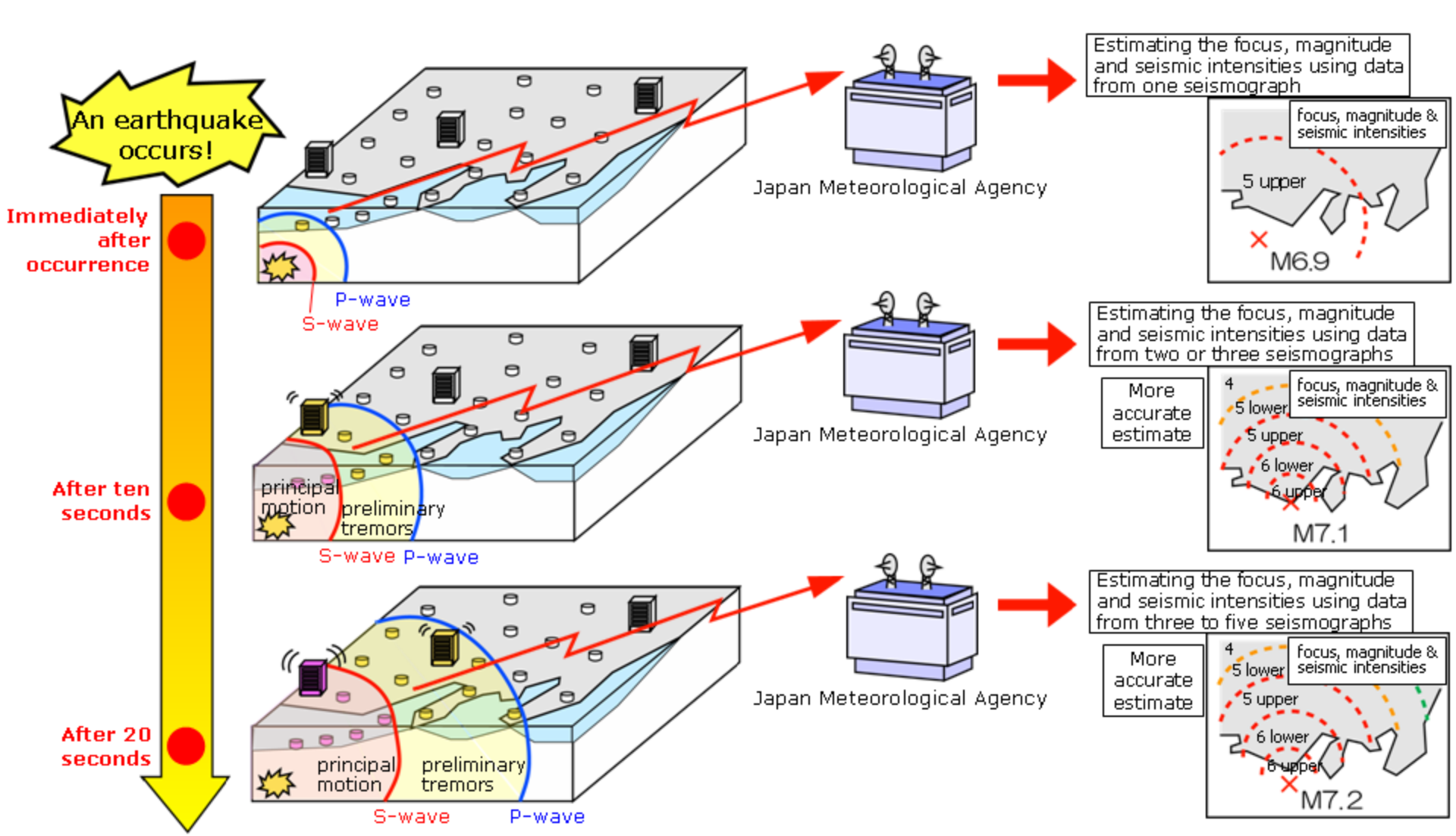

from
JMA webpage

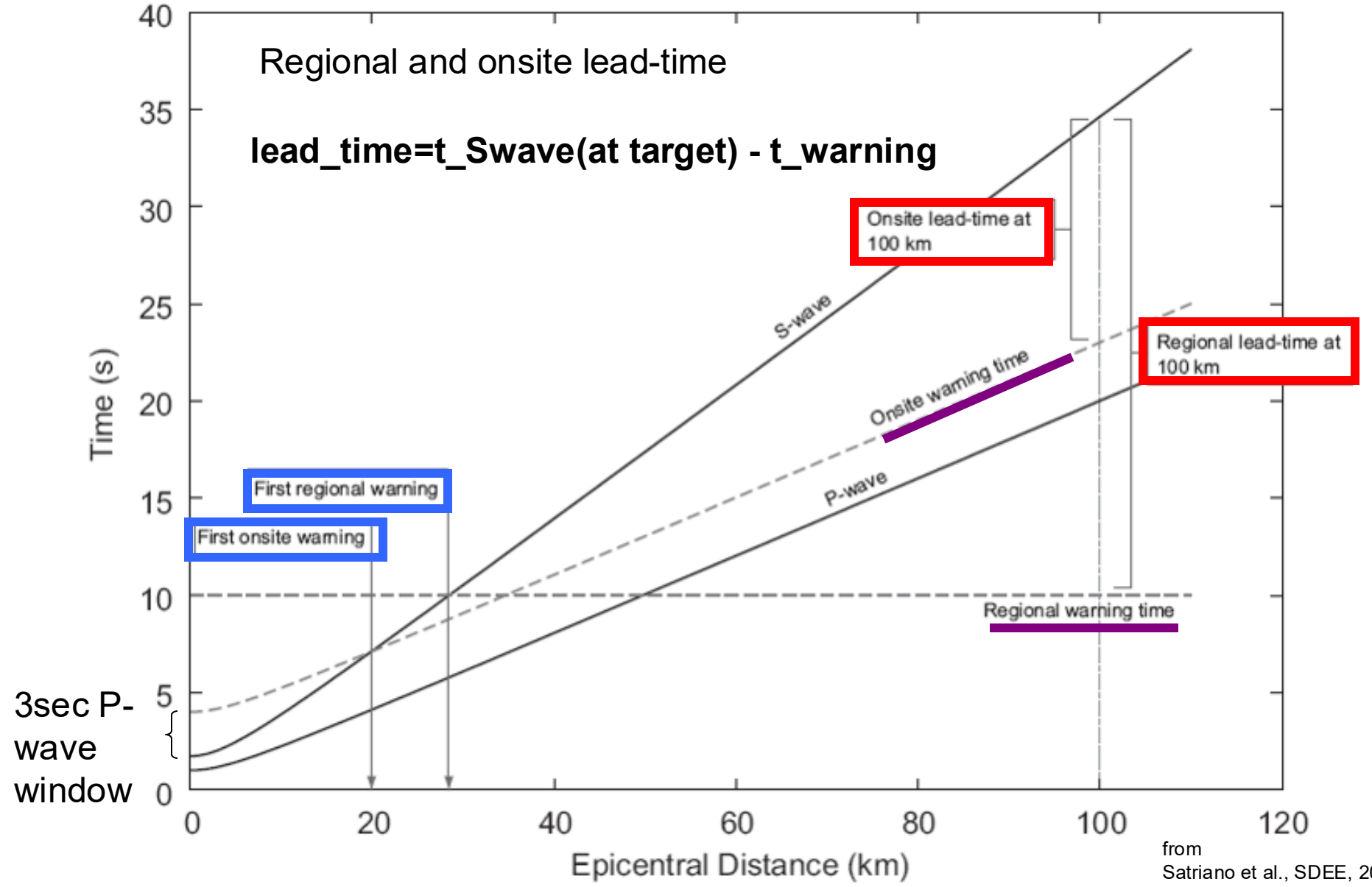

3sec P-wave window

from
Satriano et al., SDEE, 2011

Examples of estimated lead time

2008 Mw 6.9 Iwate earthquake (Japan).
lead_time=t_S-t_magnitude_estimated

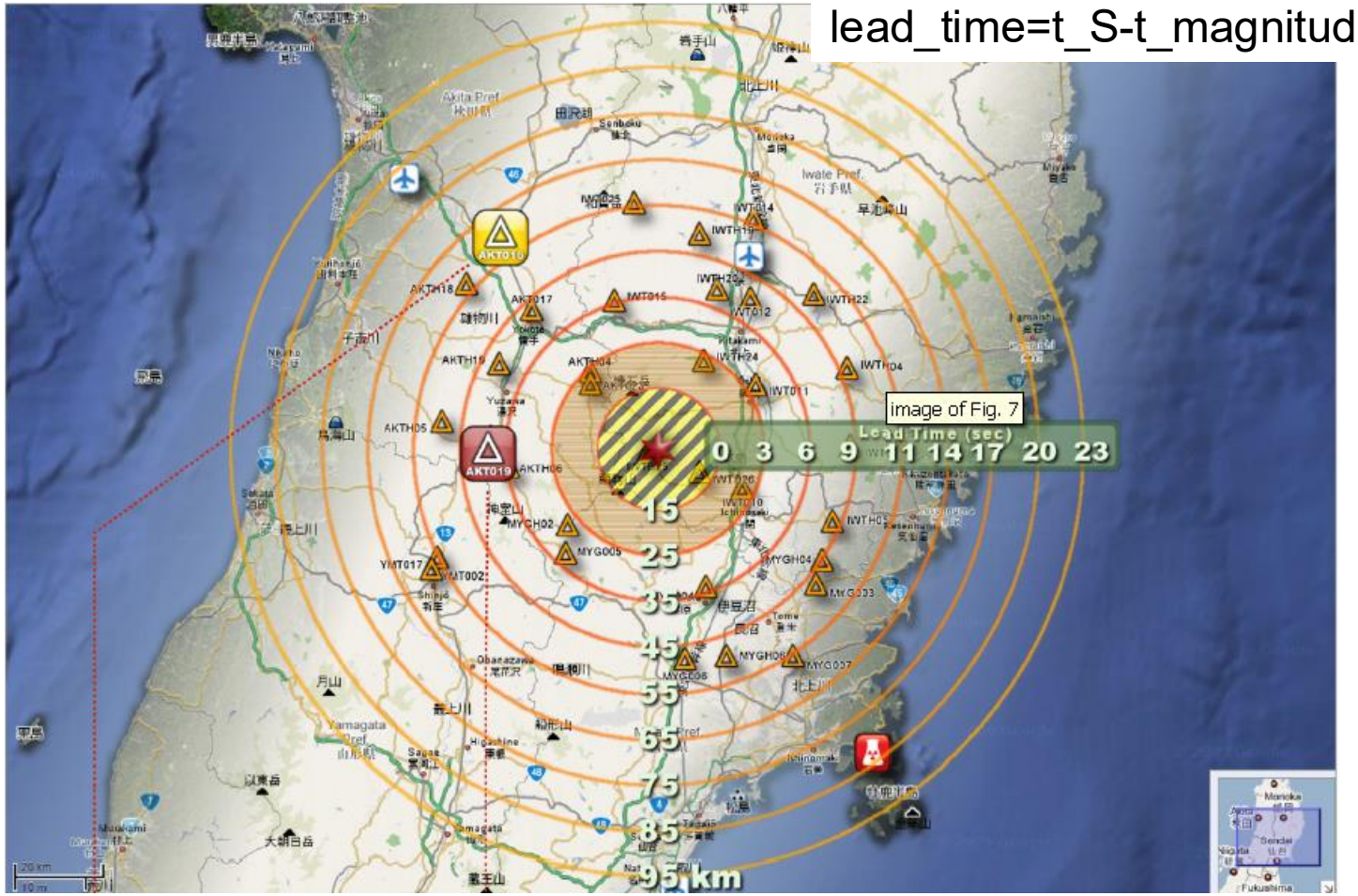

yellow:
blind zone

orange:
blind zone
when robust
magnitude
estimates are
requested

from
Satriano et al.,
SDEE, 2011

Examples of estimated lead time

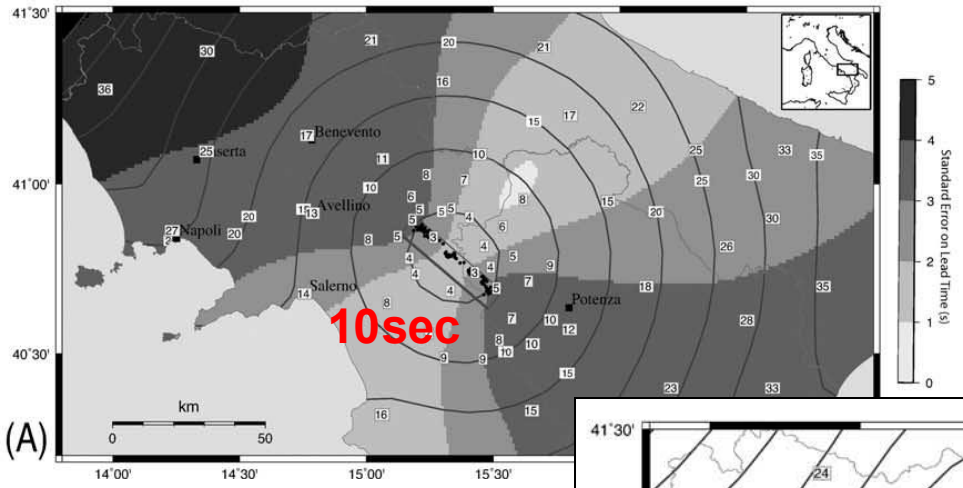

1980 Mw 6.9 Irpinia earthquake

(maximum)**lead_time**=
time_S - **time**_mag&loc_first estimate

from
Zollo et al GRL, 2009

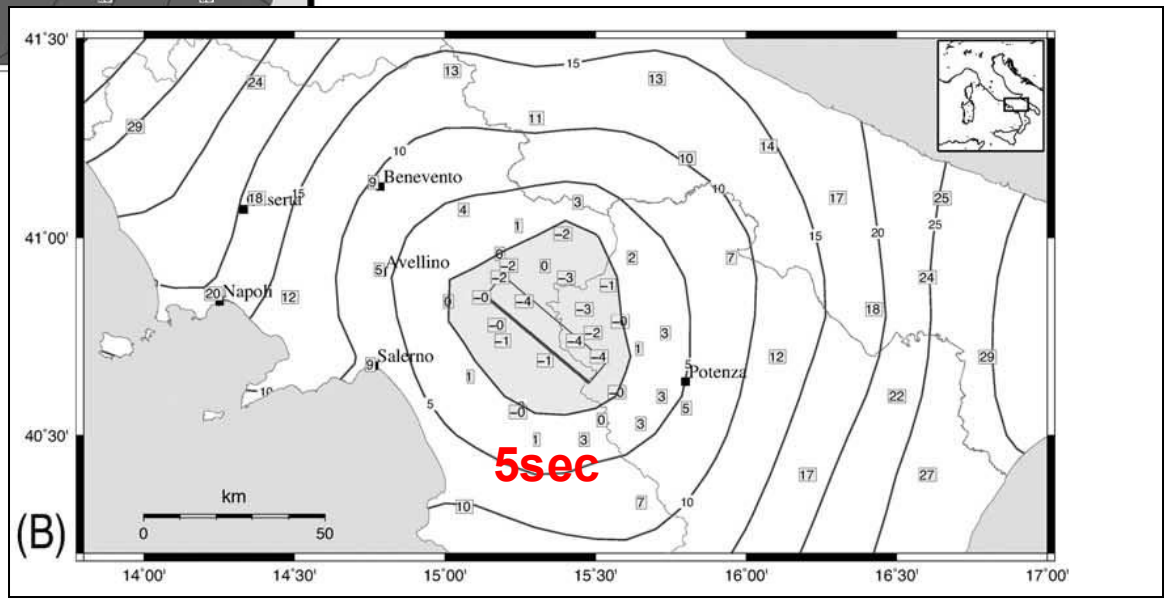

gray area:
blind zone

(effective)**lead_time=time**_S - **time**_EW_parameters_stable estimate

Examples of estimated lead time

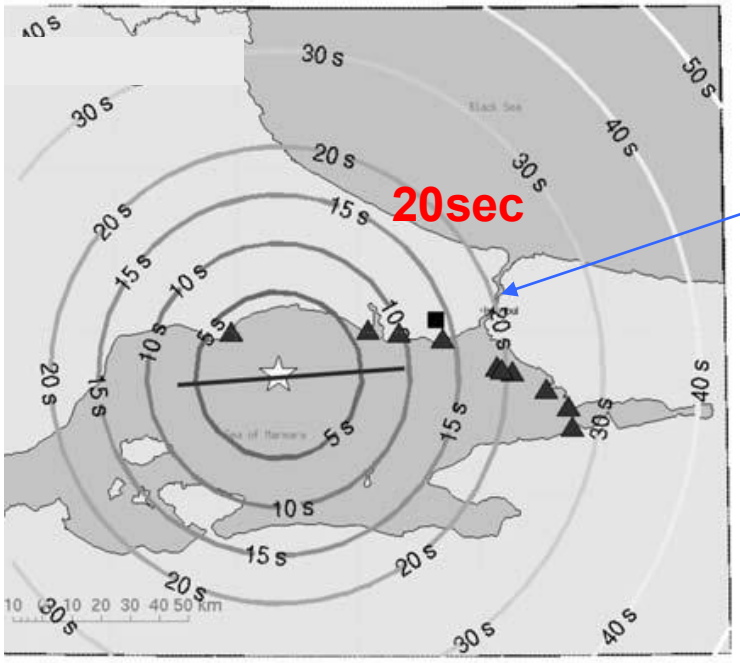

Scenario earthquake in the Marmara sea

from
Böse et al, BSSA, 2008

for this scenario earthquake the maximum lead time is 40/50 sec

Feasibility study for
Kyrgyzstan

from
Picozzi et al, JOSE, 2012

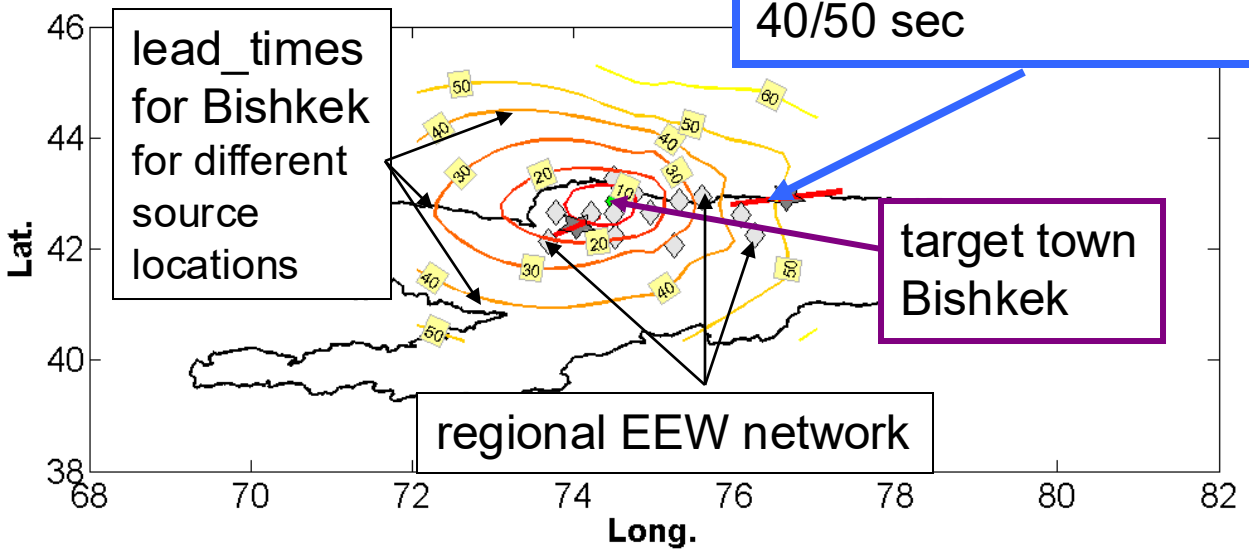

Earthquake location

Procedures for estimating early warning parameters are generally based on evolutionary (time-dependent) schemes: the “quick & dirty” estimates obtained by analyzing information gathered by a single station are constantly updated as soon as new data are acquired by the system.

Example:

ElarmS (California, Wurman et al 2007):

A) Detection based on STA(0.5sec)/LTA(5sec) ratio at each individual station.
B) Initial hypocenter placed with respect to the triggered station (depth fixed according to the regional tectonic regime).
C) When a second station is triggered, the epicenter is moved between the two stations.
D) With three or more triggers, event location and origin time are estimated using a grid search algorithm.

Earthquake location

Recently, new earthquake location procedures have been introduced.
These make use of the concept of **not-yet-triggered** stations.

Ryedelek & Pujol (2004) constrained the epicentral location using only two triggered stations and a set of not-yet-triggered ones.

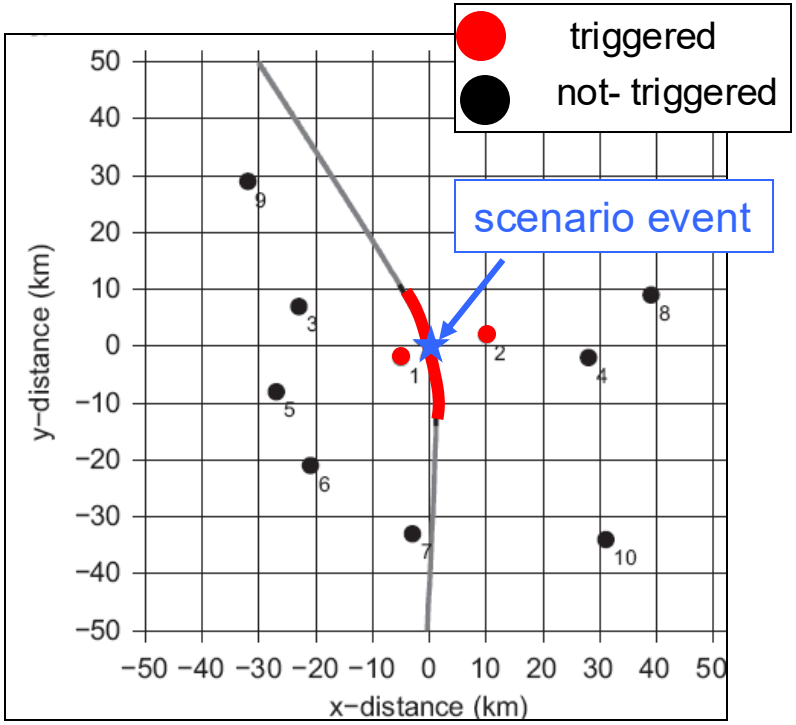

Stations 1 and 2 triggered:

$$t_2 - t_1 = \frac{1}{V}(d_2(\mathbf{x}) - d_1(\mathbf{x})) = tt_2(\mathbf{x}) - tt_1(\mathbf{x}) \qquad (1)$$

Equation (1) defines a hyperbola (open curve).
Station 3 has not yet triggered, therefore

$$\frac{1}{V}(d_3(\mathbf{x}) - d_i(\mathbf{x})) = tt_3(\mathbf{x}) - tt_i(\mathbf{x}) \geq 0, \quad i = 1,2 \qquad (2)$$

and similar inequalities can be set up for the other not-triggered stations. This set of inequalities identifies a segment (shown in red in Figure) over the hyperbola.

Earthquake location

Recently, new earthquake location procedures have been introduced. They make use of the concept of **not-yet-triggered** stations.

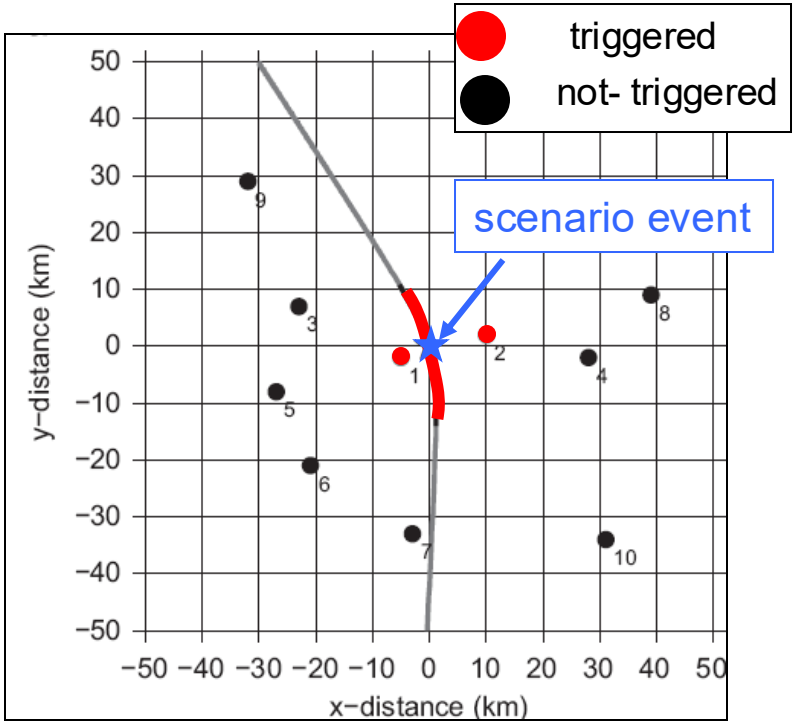

$$\frac{1}{V}(d_3(\mathbf{x})-d_i(\mathbf{x})) = tt_3(\mathbf{x})-tt_i(\mathbf{x}) \geq 0, \quad i=1,2 \qquad (2)$$

Horiuchi et al. (2005) extended this approach considering that, as time passes since the first two triggers: a) the constraint on the earthquake location given by (2) increases and b) other stations will trigger. Equation (2) can be generalized to

$$tt_j(\mathbf{x})-tt_i(\mathbf{x}) \geq t_{now}-t_i \qquad (3)$$

where i is a triggered-station and j not-trig-station. This inequalities identifies a volume containing the hypocenter which shrinks when t_now is running

Earthquake location

Cua & Heaton (2007) extended the previous approach by introducing Voronoi cells, in order to start the location determination with only one triggered station.

The approach has been further developed by Satriano et al. (2008) and Rosenberg (2009).

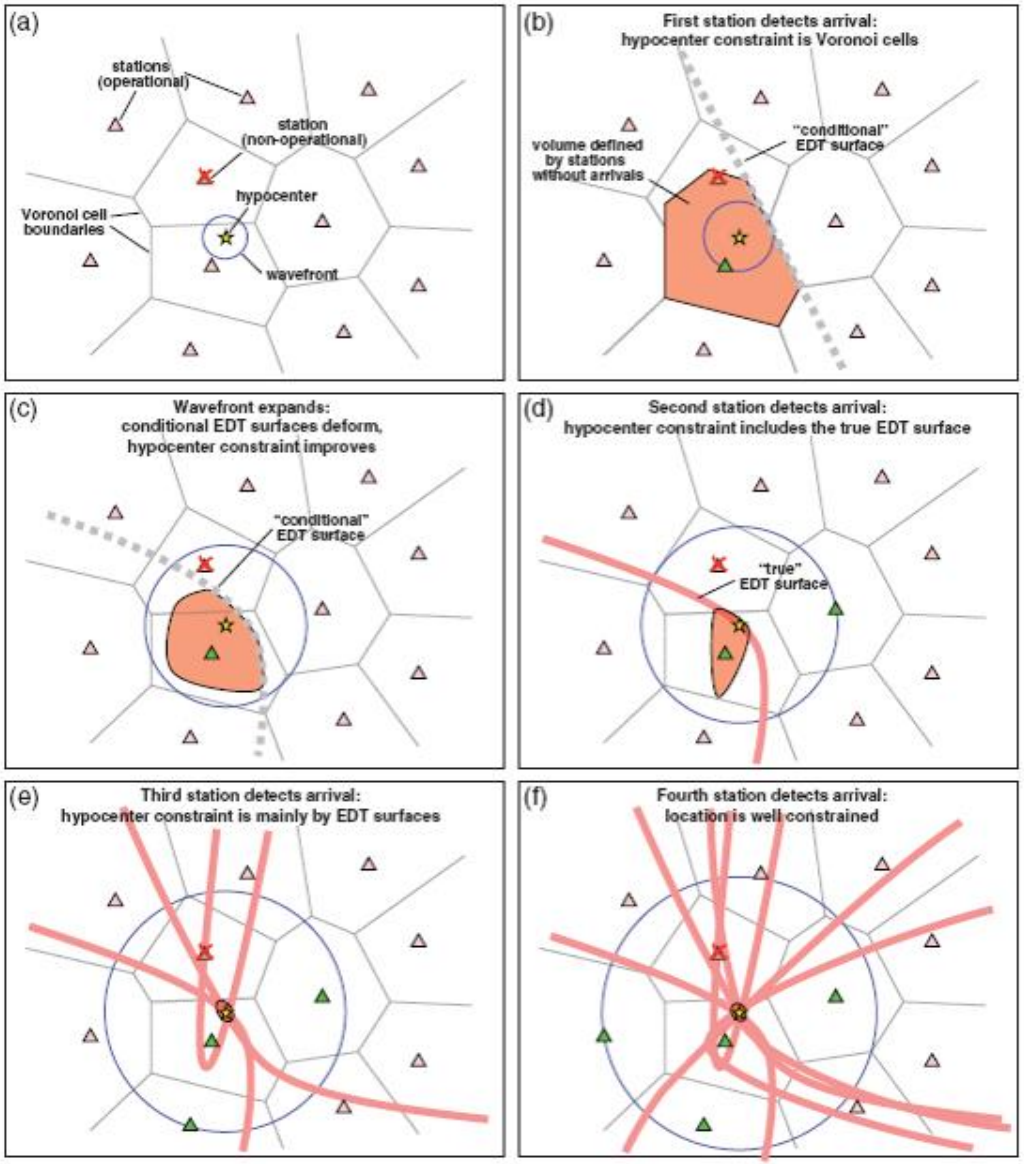

Earthquake location

Regarding the **Onsite** approaches, there are some examples of location (and magnitude) **estimation using a single station**.

Nakamura (1984). The UrEDAS system first estimates the magnitude on the basis of the predominant period of the P-waves.
Then, the hypocentral distance is inferred from the peak P-wave amplitude using an empirical magnitude-amplitude relation that includes the hypocentral distance as a parameter. The azimuth of the epicenter is determined by polarization analysis over the three components.

Odaka et al (2003). The function
B t *exp*(-A t) is fitted to the envelope of the vertical component of acceleration (considering the first 3 sec). It has been observed that log(B) is proportional to – log(distance). The distance is first found using the measured B value, then the magnitude is determined using empirical equations for P-wave amplitude as in the Nakamura method.

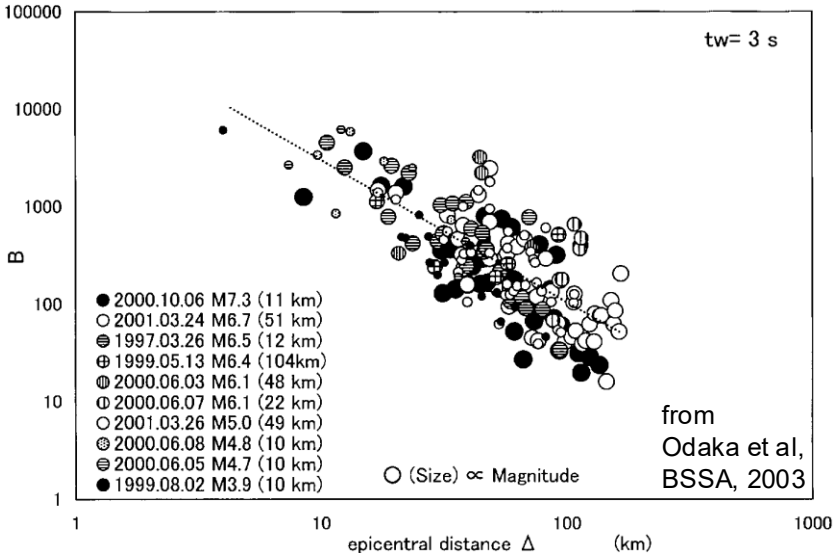

Earthquake location

Böse et al (2012). The **PreSeis On-site** approach provides a rapid earthquake/noise discrimination, a near/far source classification, and estimates the moment magnitude, the epicentral distance, and the peak ground velocity at the site of observation. PreSeis uses the seismic acceleration, velocity, and displacement waveforms recorded at a single three-component Strong Motion (SM) or Broad-Band (BB) sensor. The algorithm is based on Artificial Neural Networks (ANNs). Moreover, it uses global data sets of BB and SM records for the training phase. This makes the approach more general and less linked to a specific region.

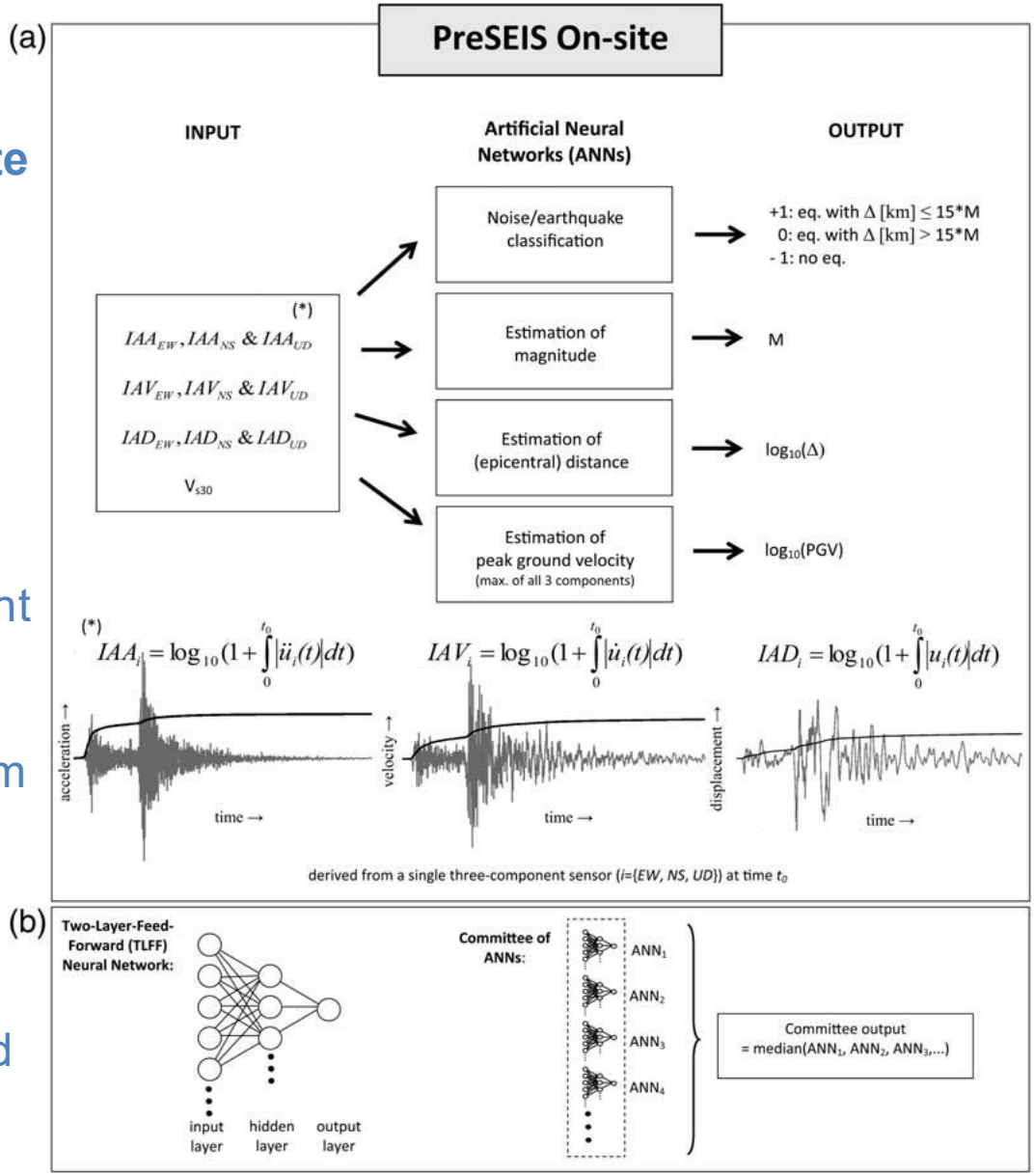

Earthquake magnitude estimation

Rapid magnitude estimation for EEW is based on the observation that quantities like peak displacement, characteristic period, etc., estimated in the first few seconds of the recorded P- or S-signal, can be correlated to the final earthquake size. The EEW magnitude estimation is therefore based on empirical relationships between early-measured parameters and the earthquake's size.

from
Satriano et al., SDEE, 2011

Examples:

The use of the initial portion of recorded P-wave for magnitude determination was introduced by Nakamura (1988). The **predominant period** is computed from the initial 2-4 sec of P-wave. It is called τ_p after Allen and Kanamori(2003). It is computed in real time from the vertical component of velocity (V) and acceleration (A):

$$\tau_{p,i} = 2\pi\sqrt{\frac{V_i}{A_i}}$$

where

$$V_i = \alpha V_{i-1} + v_i^2$$

$$A_i = \alpha A_{i-1} + a_i^2$$

and a is a smoothing parameter from 0 and 1.

Earthquake magnitude estimation

Nakamura (1988) and Allen and Kanamori(2003) observed that the predominant period linearly scales with the earthquake size.
Kanamori (2005) introduced the parameter τ_c which is similar to τ_p but defined as

$$r = \frac{\int_0^{\tau_0} \dot{u}^2(t)\,dt}{\int_0^{\tau_0} u^2(t)\,dt} \qquad \tau_c = \frac{1}{\sqrt{\langle f^2 \rangle}} = \frac{2\pi}{\sqrt{r}}$$

With τ_0 generally equal to 3 sec, and with displacement obtained by numerical integration and high-pass filtered at 0.075 Hz.

The effectiveness of this approach is still under debate.

Earthquake magnitude estimation

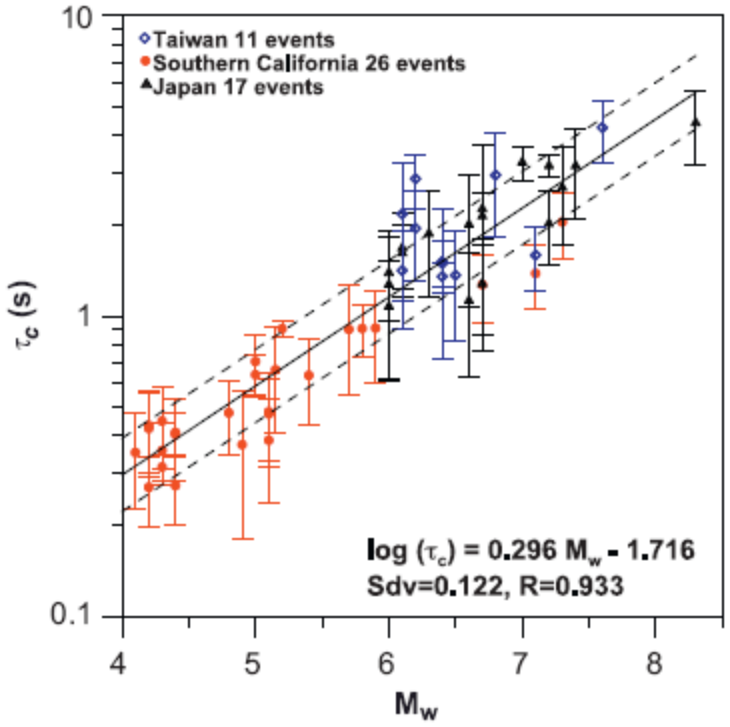

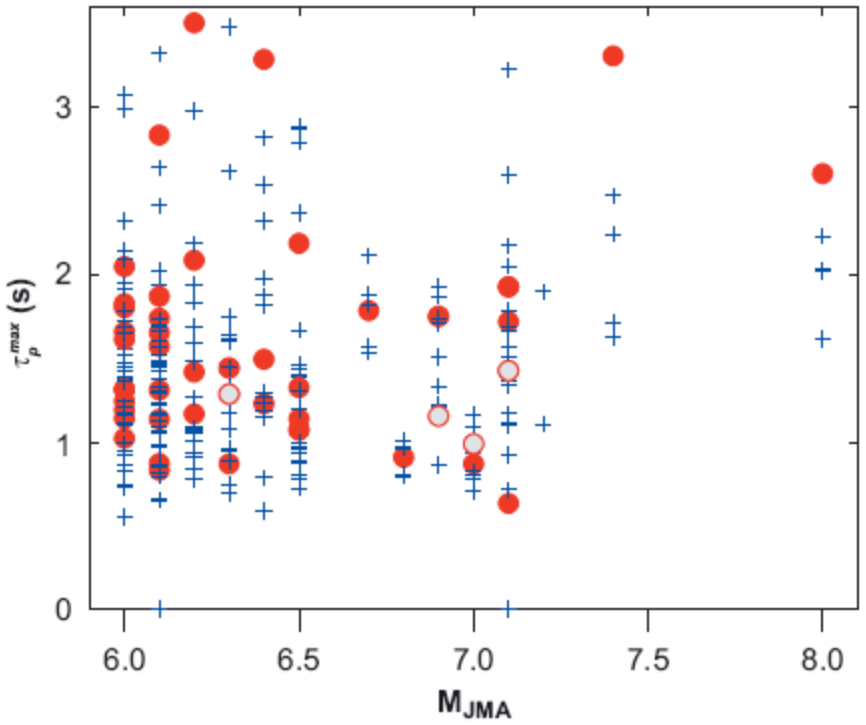

Wu and Kanamori (2008): Correlation between τ_c and Mw of earthquakes in Japan, Southern California, and Taiwan.

Rydelek and Horiuchi (2006): No-Correlation is seen between τ_p and M_{JMA} of earthquakes in Japan (Hi-Net)

from
Satriano et al., SDEE, 2011

Earthquake magnitude estimation

Different parameters from the predominant period have been introduced.
Wu & Zhao(2006) and Zollo et al. (2006) investigated the peak displacement amplitude measured on the early P (and S) phases.
Wu and Zhao called this parameters Pd, measured on the vertical component, using the first 3 sec after the P arrival. They studied the attenuation of Pd with magnitude and distance in southern California:

$$\log P_d = A + BM + C \log R$$

where the constants A, B, and C are determined trough regression analysis for the studied area. Once the distance is determined by the EEW algorithm, this empirical model is used to estimate M from the measured Pd.

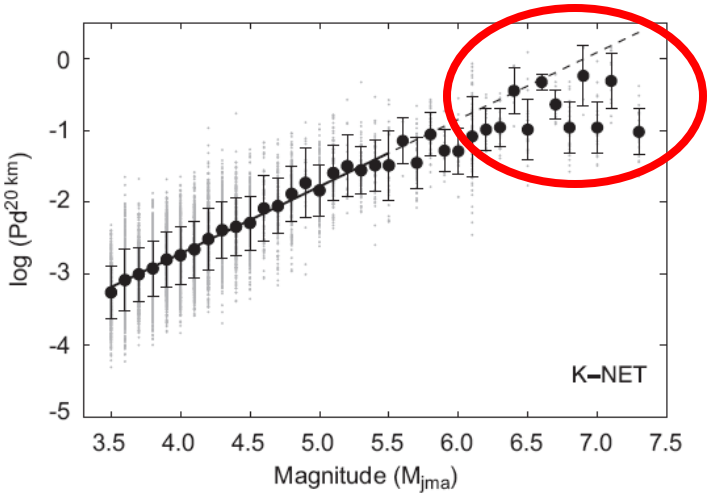

The saturation effect is removed by considering larger windows (4sec of P-wave) or using the peaks read from the S-waves (Zollo et al, 2996; Lancieri and Zollo, 2008).

from
Satriano et al., SDEE, 2011

Earthquake magnitude estimation

Another class of EEW parameters used for estimating the earthquake size involves **integral measurements** (e.g. Festa et al., 2008)

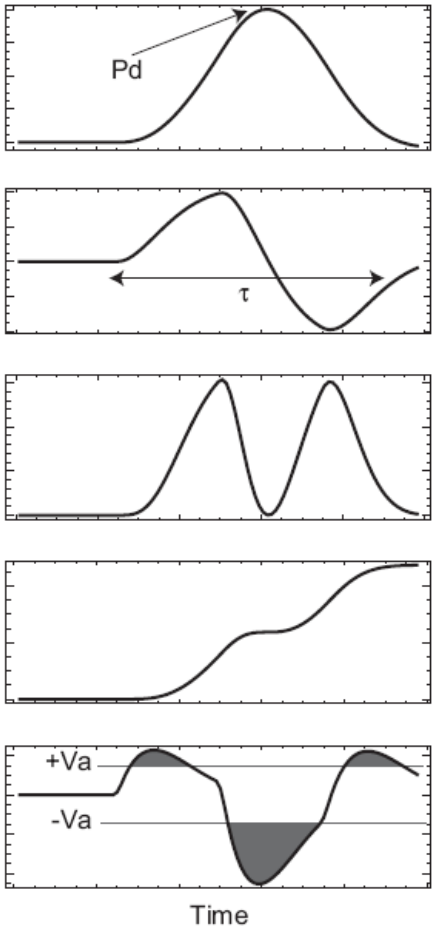

Displacement — **Peak**

Velocity — **Predominant period**

V^2 or |A| — **Integral**

IntV^2 or CAV — **Integral**

Acceleration — **Average peak**

from
Satriano et al., SDEE, 2011

$$CAV = \int_0^{t_{max}} |a(t)|\, dt$$

$$IV2_c = \int_{t_c}^{t_c + \Delta t_c} v_c^2(t)\, dt$$

with c= P or S phases

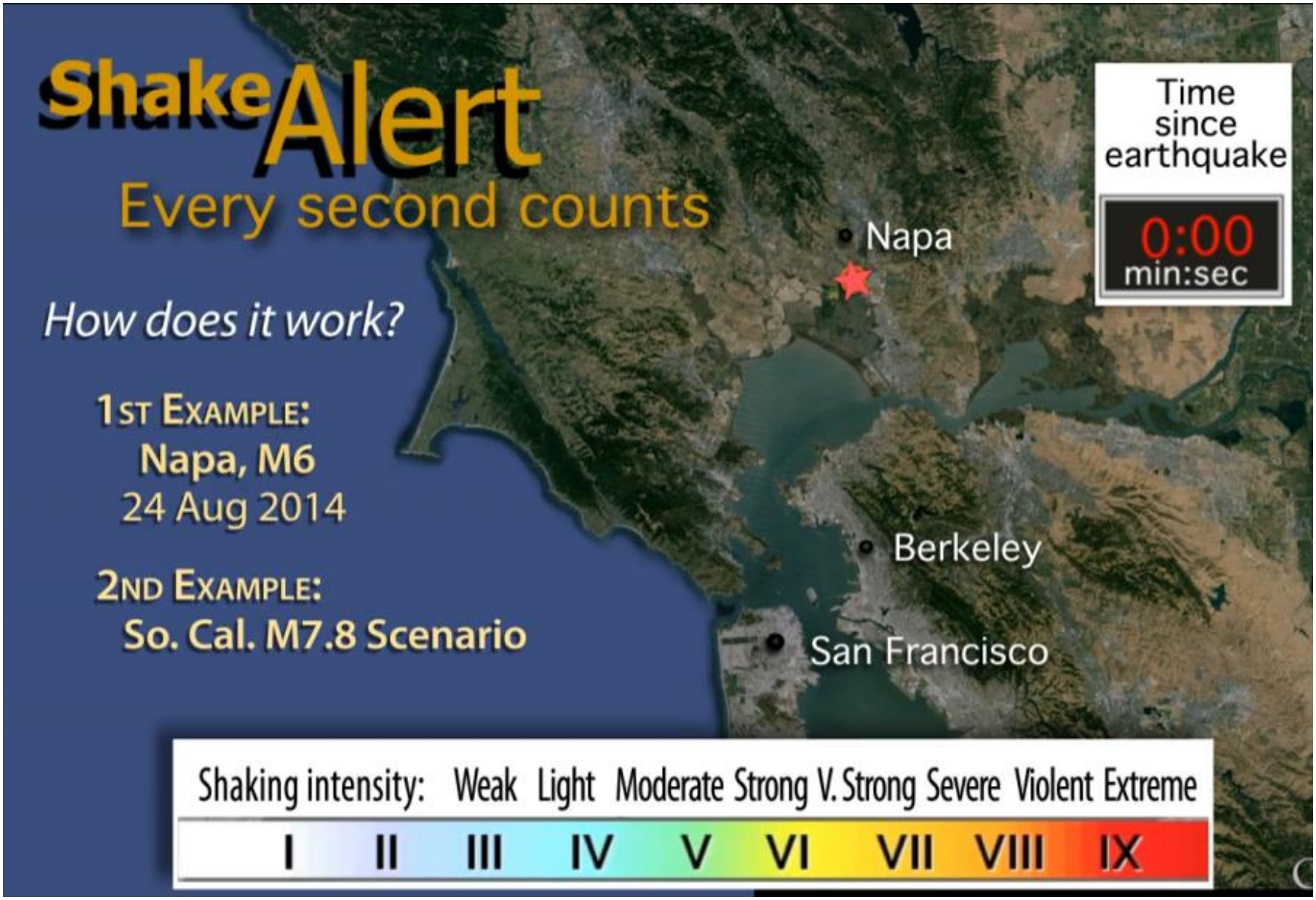
ShakeAlert
Every second counts
How does it work?
1ST EXAMPLE:
Napa, M6
24 Aug 2014
2ND EXAMPLE:
So. Cal. M7.8 Scenario
Napa
Berkeley
San Francisco
Time since earthquake
0:00
min:sec
Shaking intensity: Weak Light Moderate Strong V. Strong Severe Violent Extreme
I II III IV V VI VII VIII IX

Decentralised Onsite Early warning

Real-time acceleration

Event detection

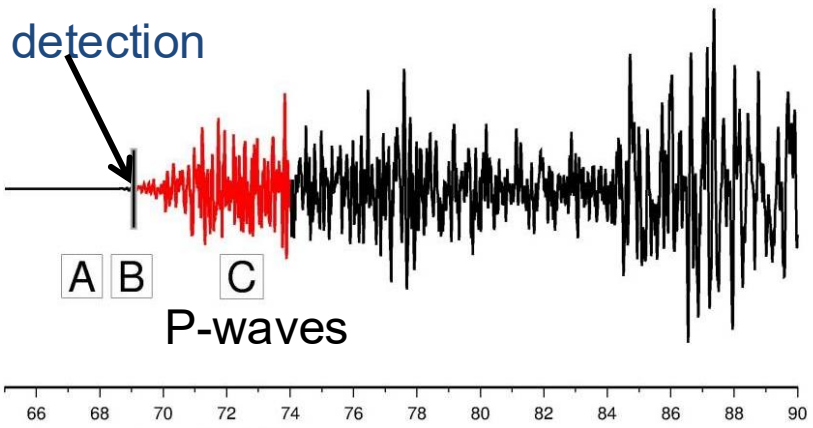

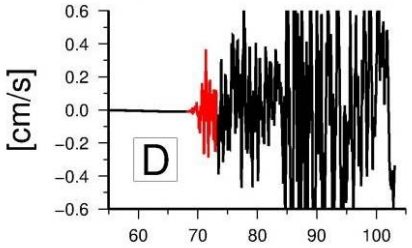

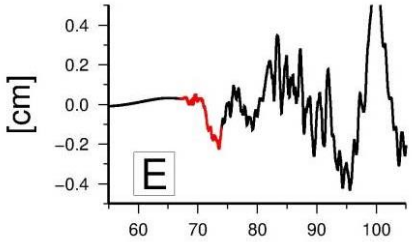

F

Empirical model

logPGV(S)=a+b*logPGD(P)

from early P–wave (measurement)

to S–wave (prediction)

Peak Displacement over 3s P-wave

Alert protocols based on PGV thresholds & expected damage levels

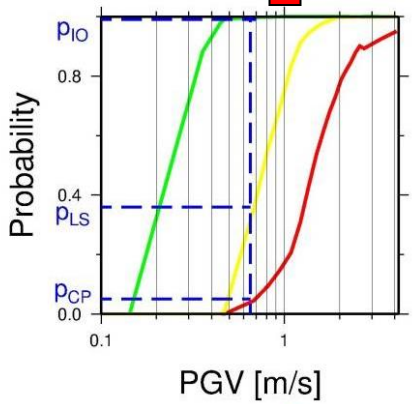

Alert protocols based on PGV thresholds

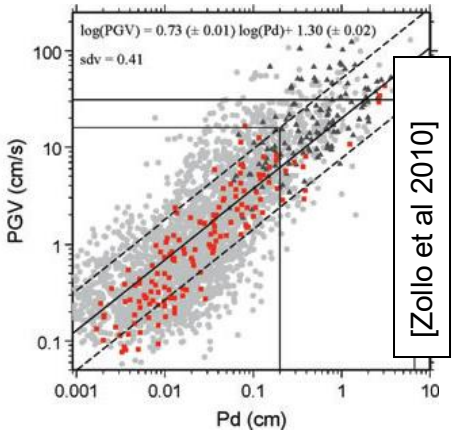

[Zollo et al 2010]

http://www.dspguide.com/CH19.PDF

Online application to Kyrgyzstan: Lead time for Bishkek

ACROSS Network

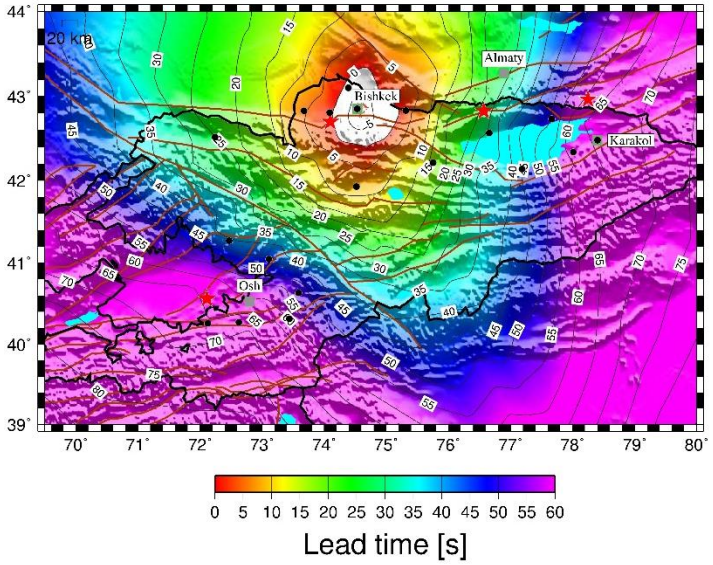

DOSEW

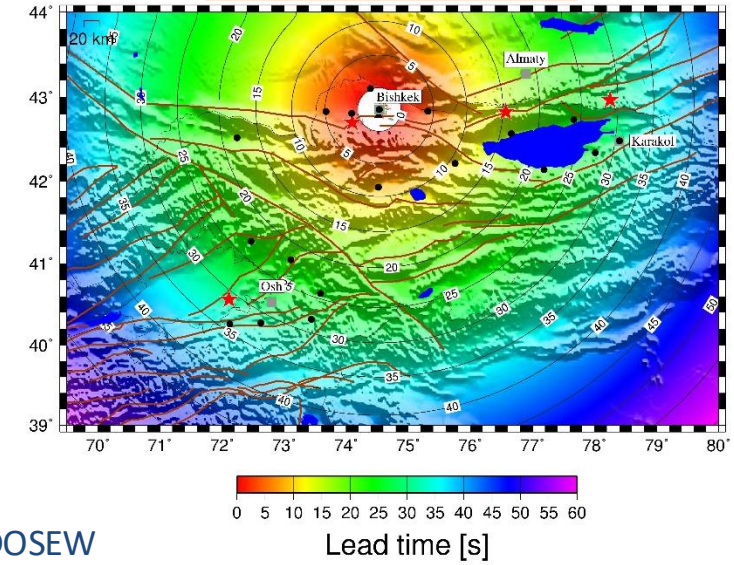

ACROSS + DOSEW

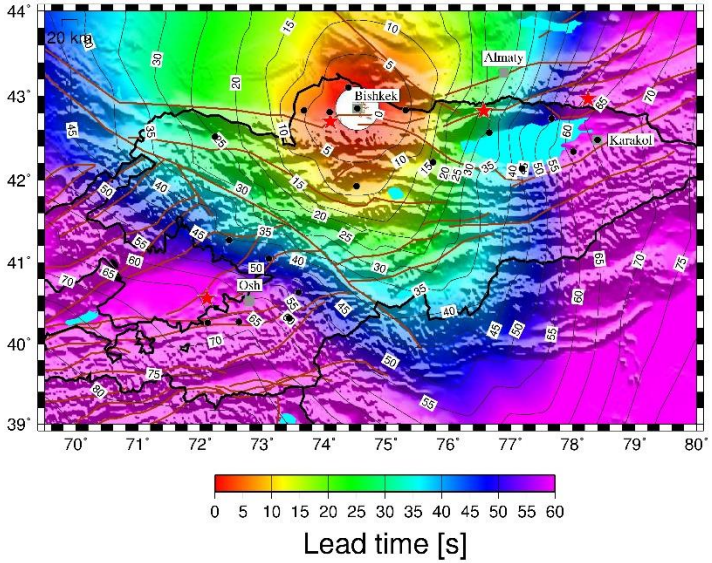

The **Presto** (Regional) and **GFZ-Sentry** (Decentralised on Site) softwares are running in a testing phase on the network

from
Parolai et al.,2017, Frontiers

Are magnitude and location necessary?

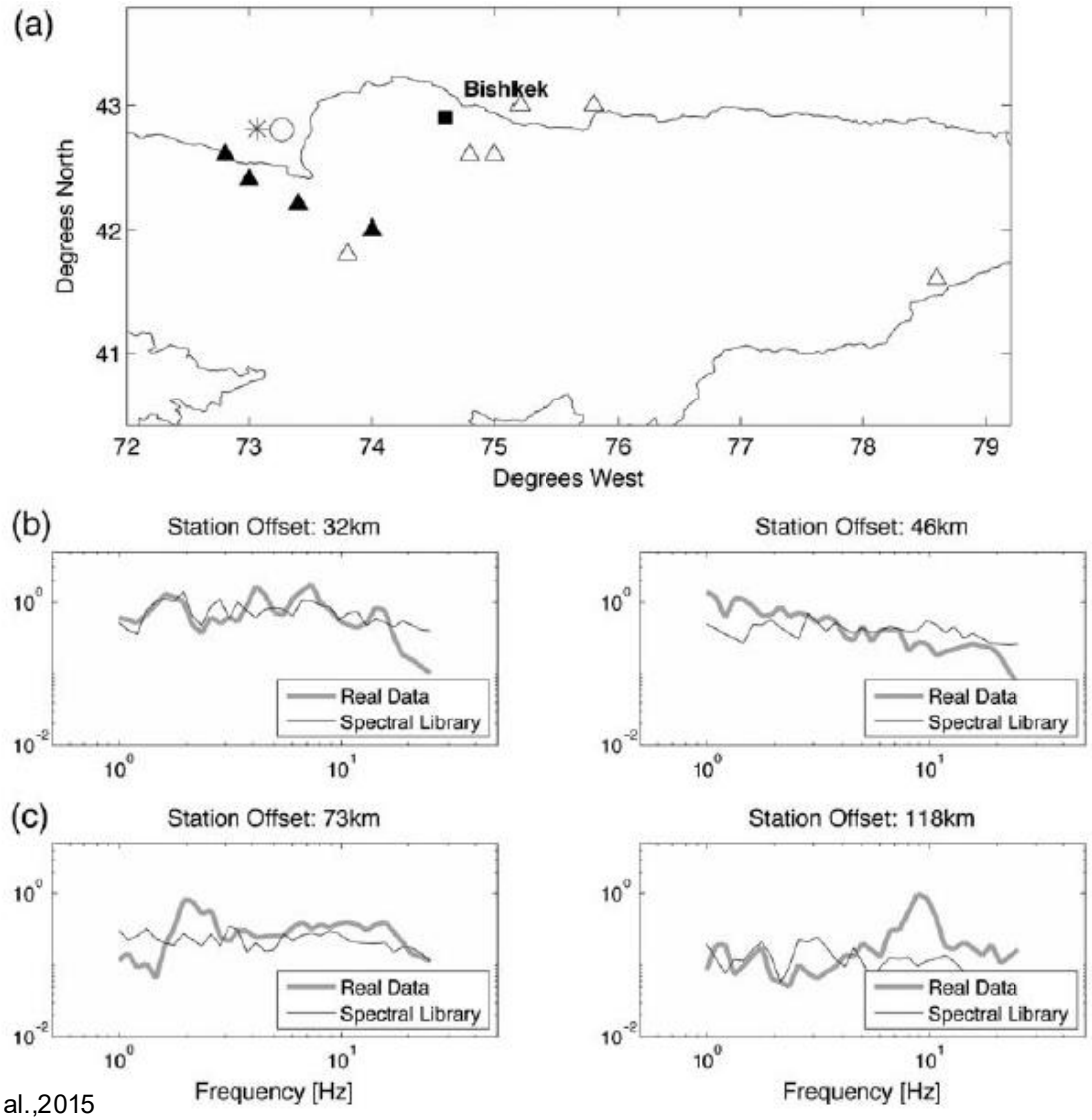

from
Stankiewicz et al.,2015

Spectral content used to improve Earthquake Early Warning Systems Bishkek

Timely warning than was possible using a threshold on ground motion

Improvement should come from a **combination with On-Site Early Warning**

Some Emerging questions

How to deal with nearly simultaneous aftershocks?
How to include site effects in real time shaking forecasting?

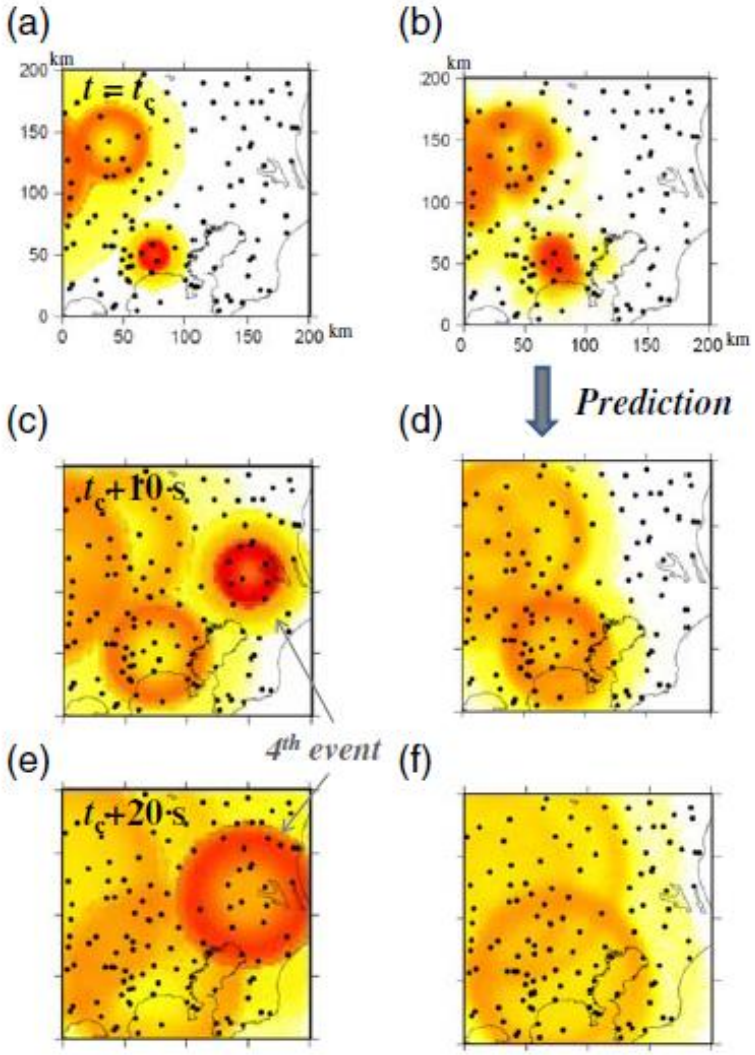

Hoshiba and Aoki (2015):

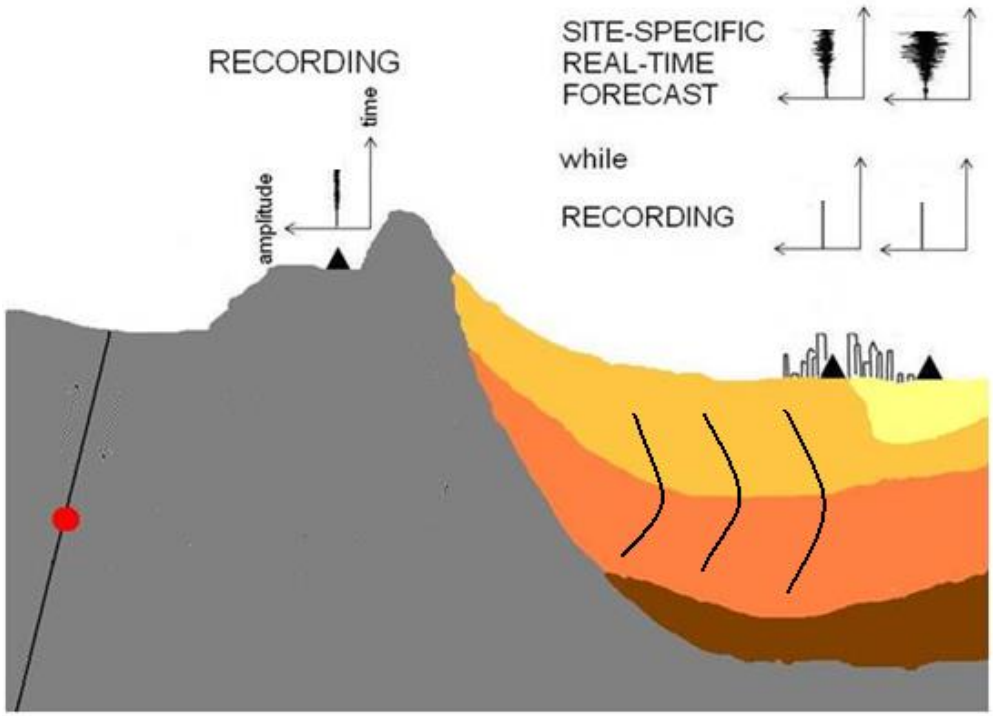

Pilz and Parolai (2016), Hoshiba (2020)

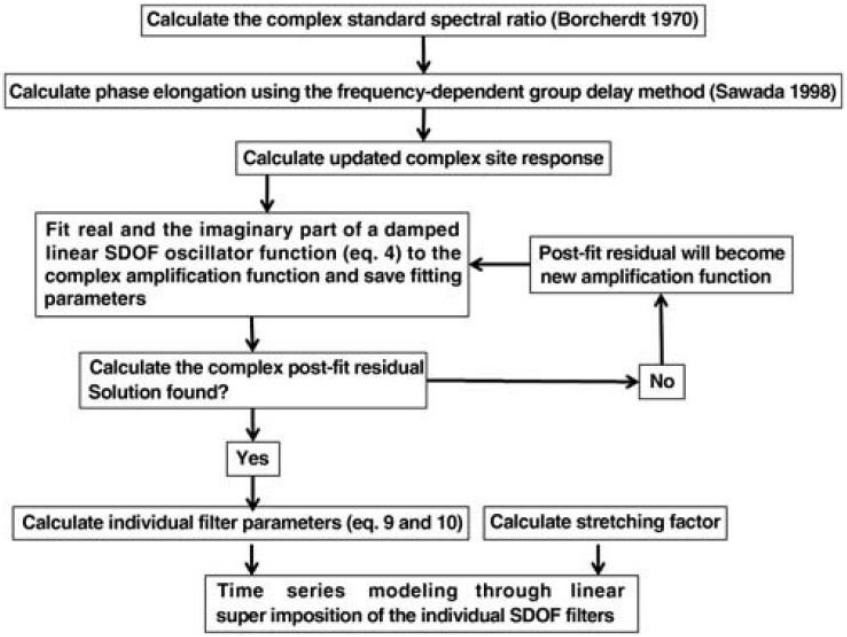

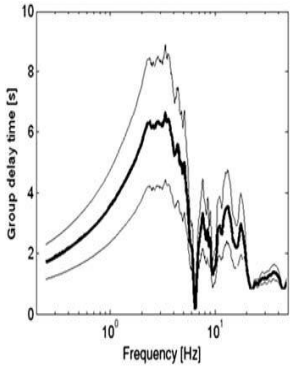

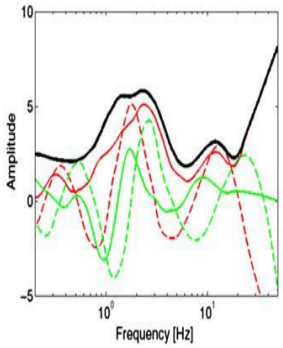

Reference

stretched

+ site

observed

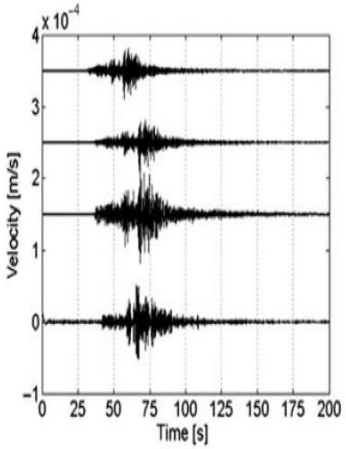

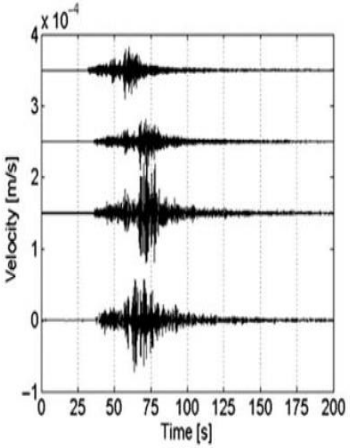

Reference

stretched

+ site

observed

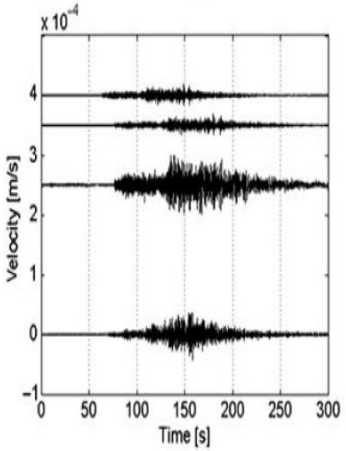

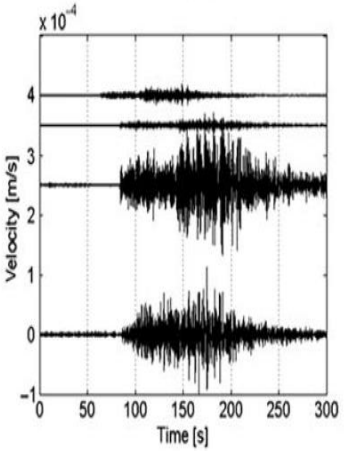

Emerging questions

Aftershocks early warning and monitoring: time dependent vulnerability

Non structural damage: Induced seismicity

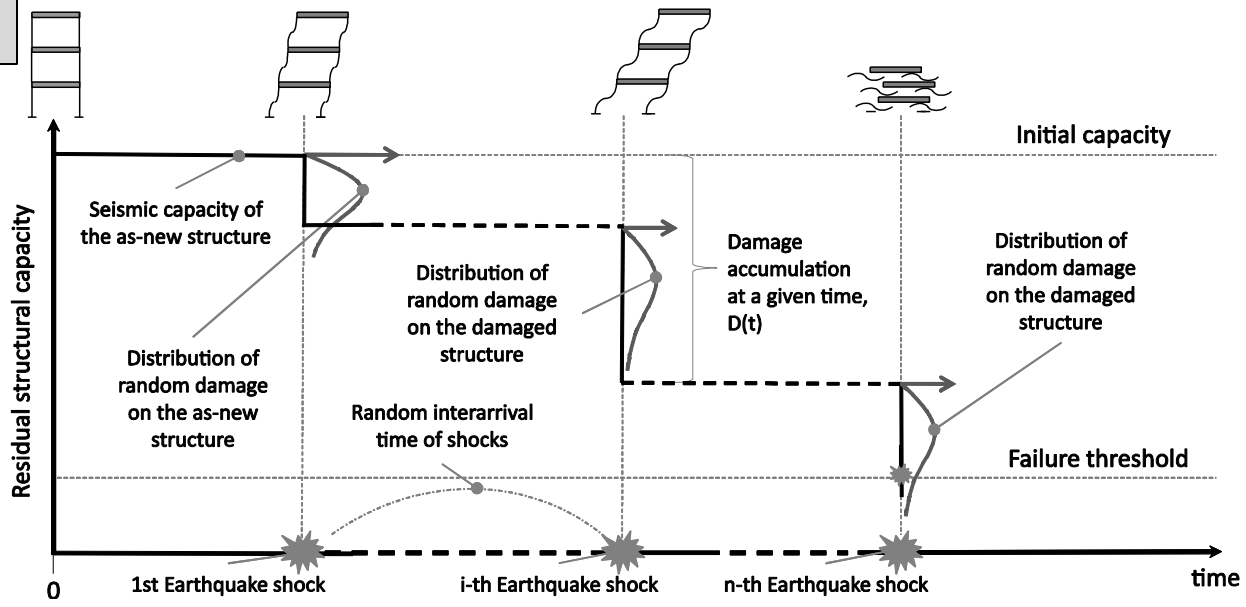

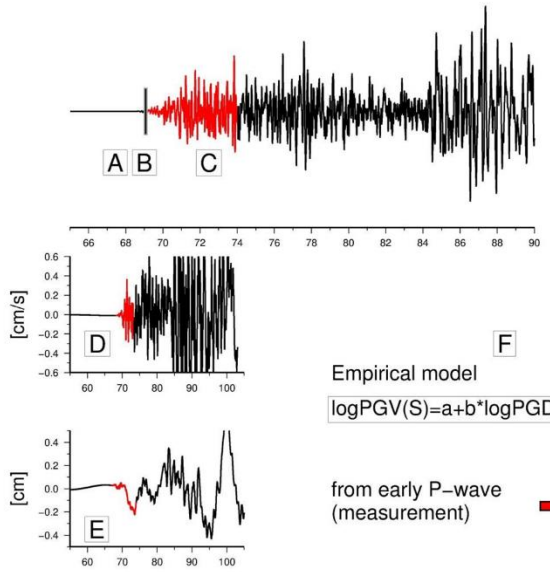

Empirical model

logPGV(S)=a+b*logPGD(P)

from early P–wave (measurement) → to S–wave (prediction)

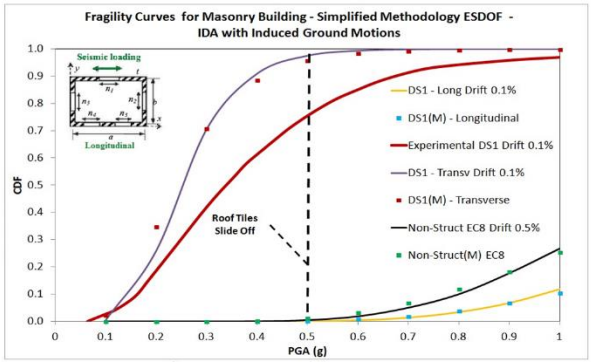

Developed for Drift Sensitive Brittle Non-Structural Components of URM buildings.

MP-Wise (Multi-Parameter Wireless Sensing System)

Applications

ACROSS Network

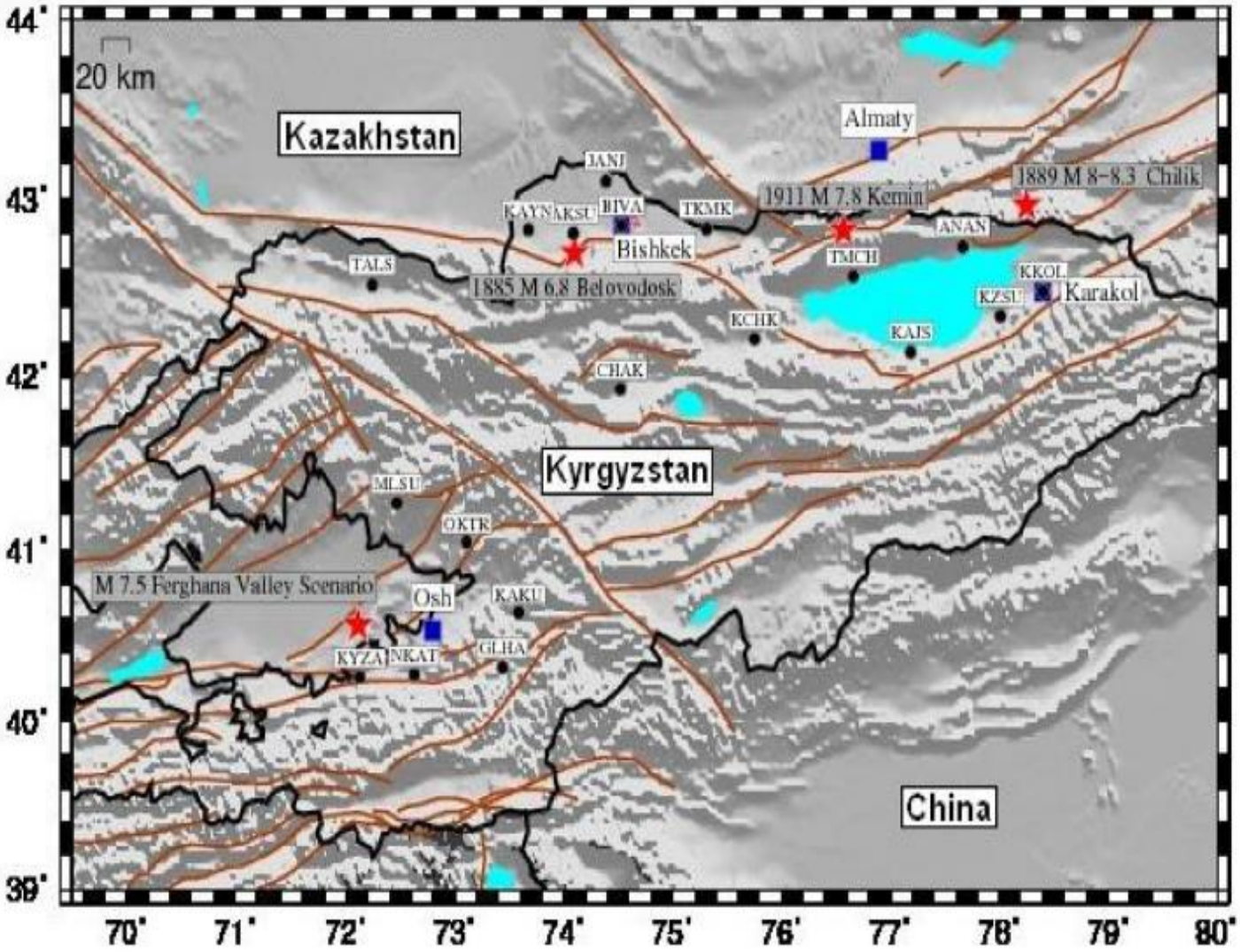

1887 Verny Earthquake M=7.3

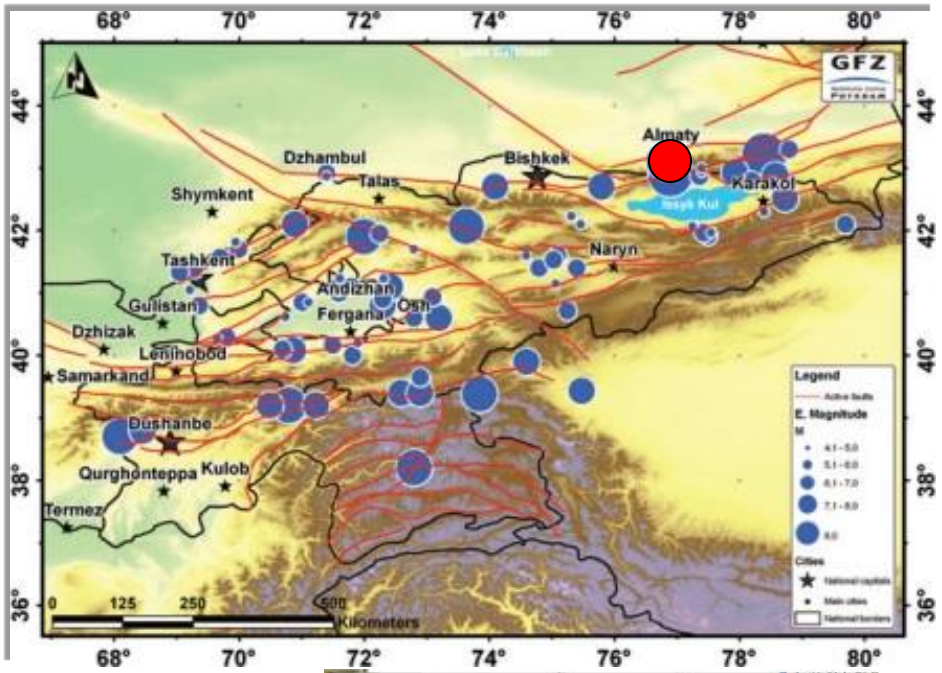

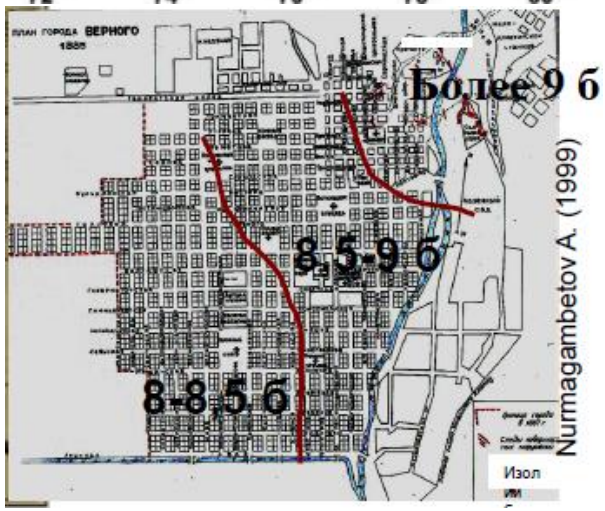

Macroseismic Intensities in Almaty

~300 death

Nurmagambetov (1999)

Nurmagambetov (1999)

1911 Kemin Earthquake M=7.8-8.0

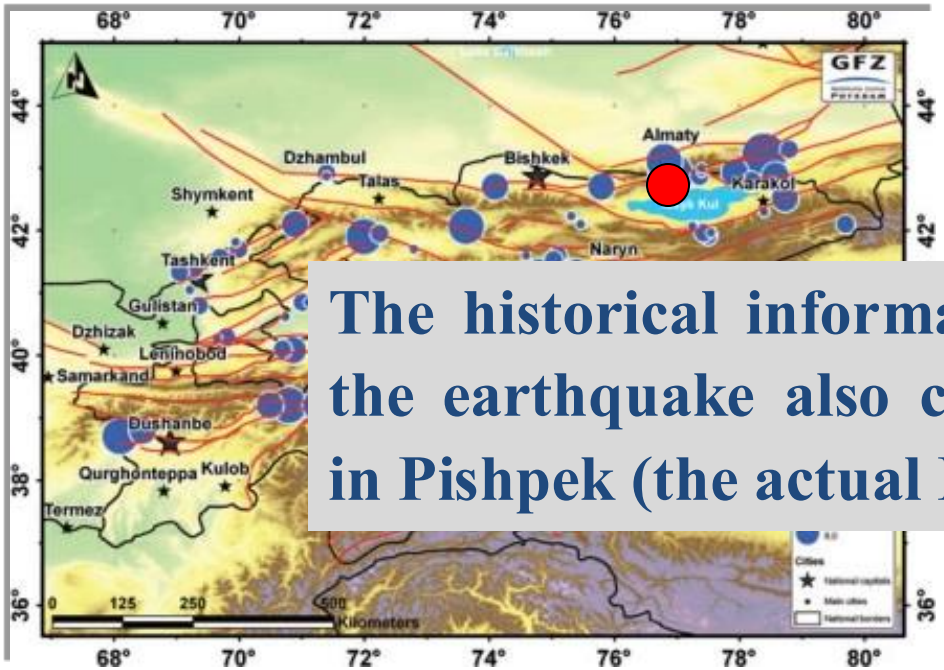

The historical information suggests that the earthquake also created devastation in Pishpek (the actual Bishkek)

Almaty

Nurmagambetov (1999)

Macroseismic Intensities in Almaty

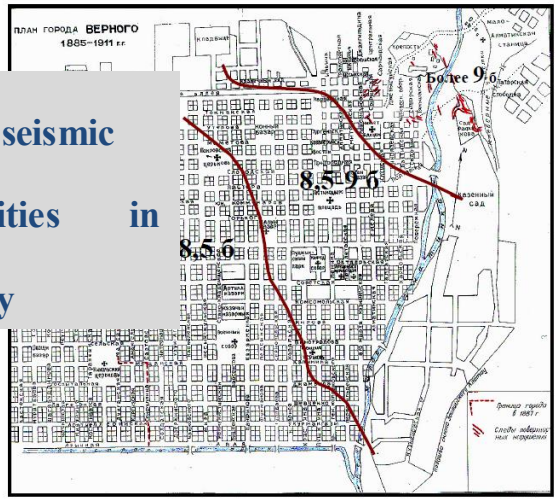

Almaty

Nurmagambetov (1999)

Nurmagambetov (1999)

High risk considering the urban dynamic

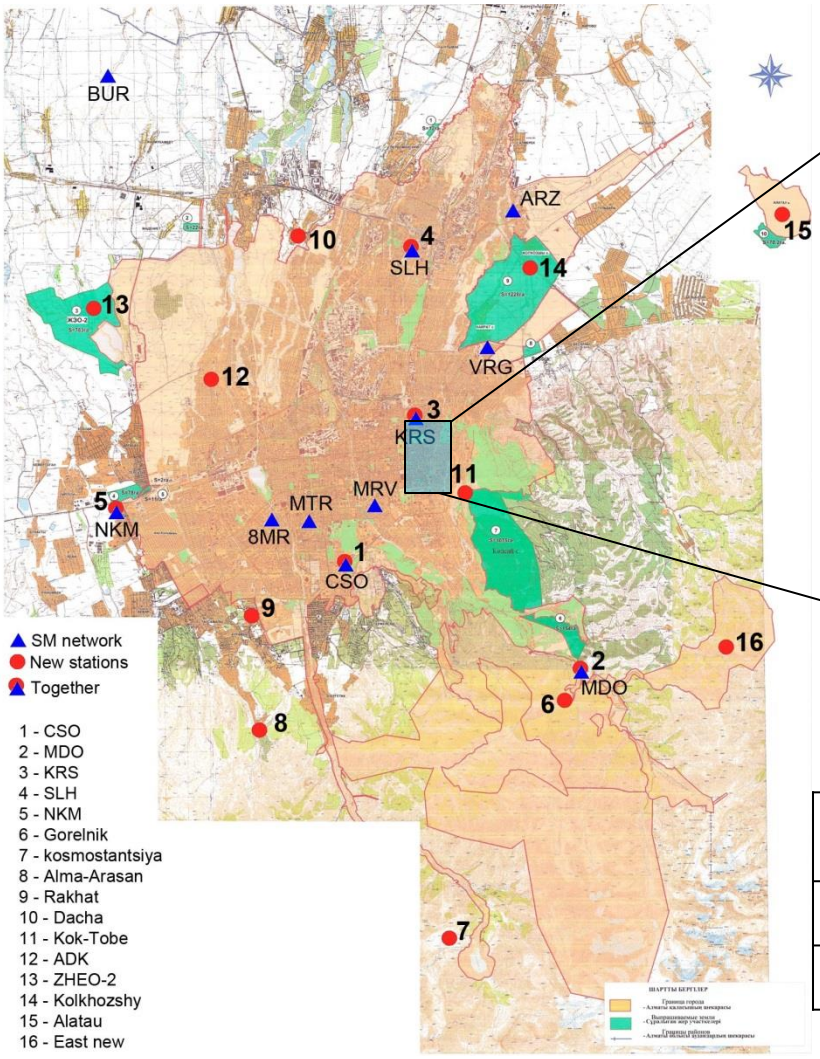

Parolai et al (2018) in preparation

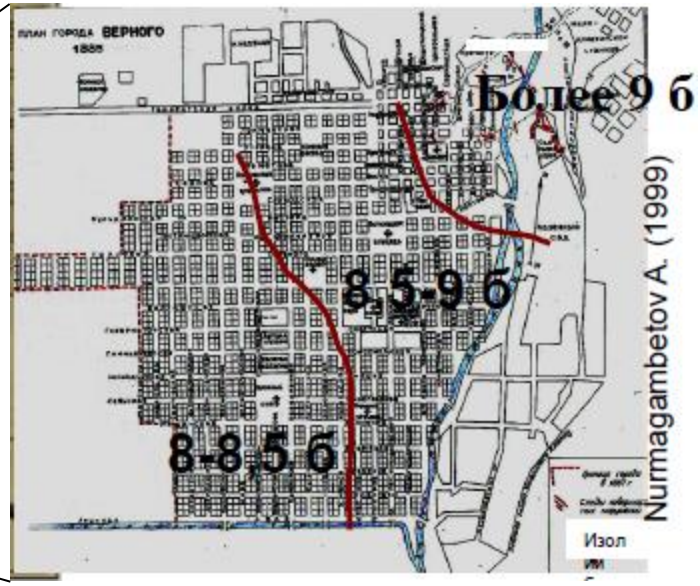

City	Population (millions)	Estimated deaths (thousands)	Estimated Injuries (thousands)
Almaty	1.5	75	300
Bishkek	0.8 (now ~1)	40	160

GeoHazards Int. B.Tucker, pers. comm.

Earthquake risk early warning

Picozzi et al (2013)

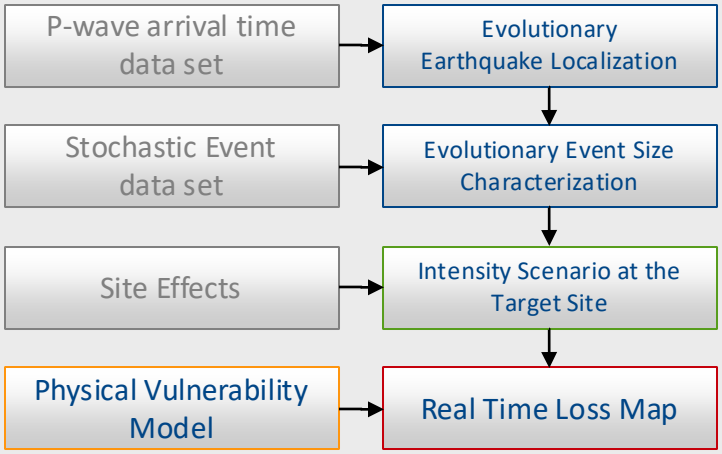

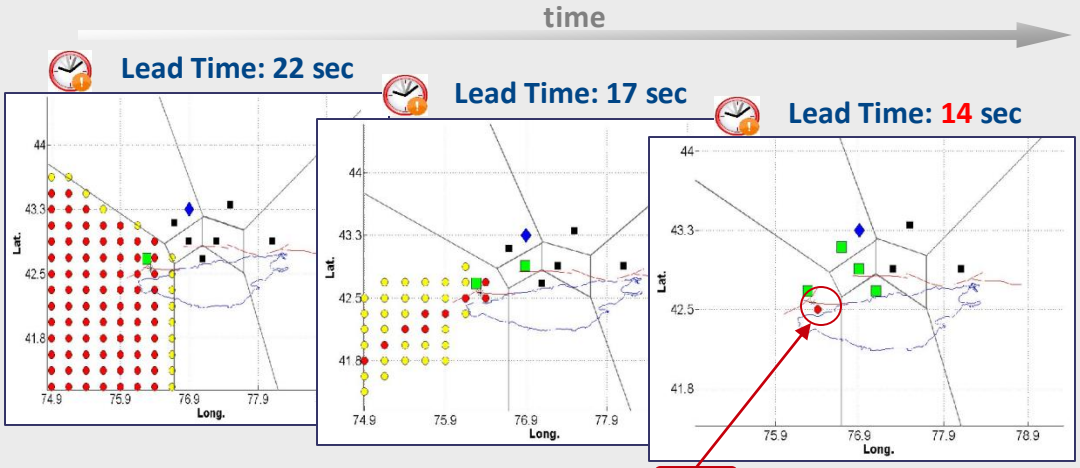

Real-time loss scenario filtering

Event characterized, most probable scenario selected, warning

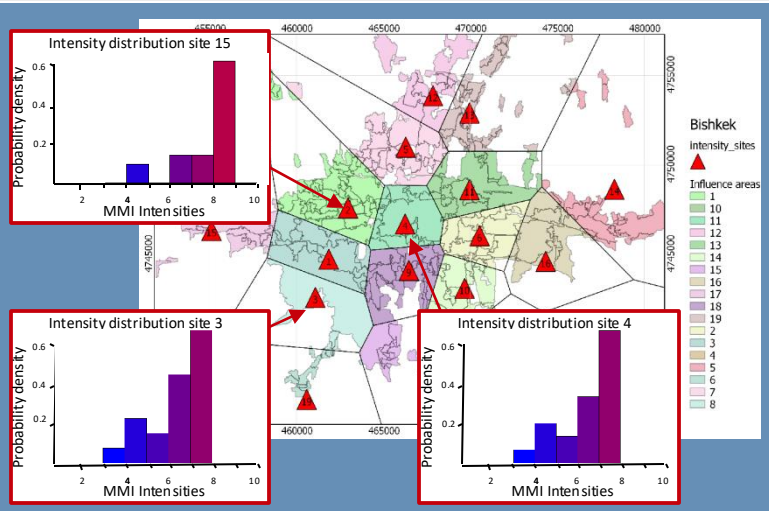

Spatial distribution of simulated intensity

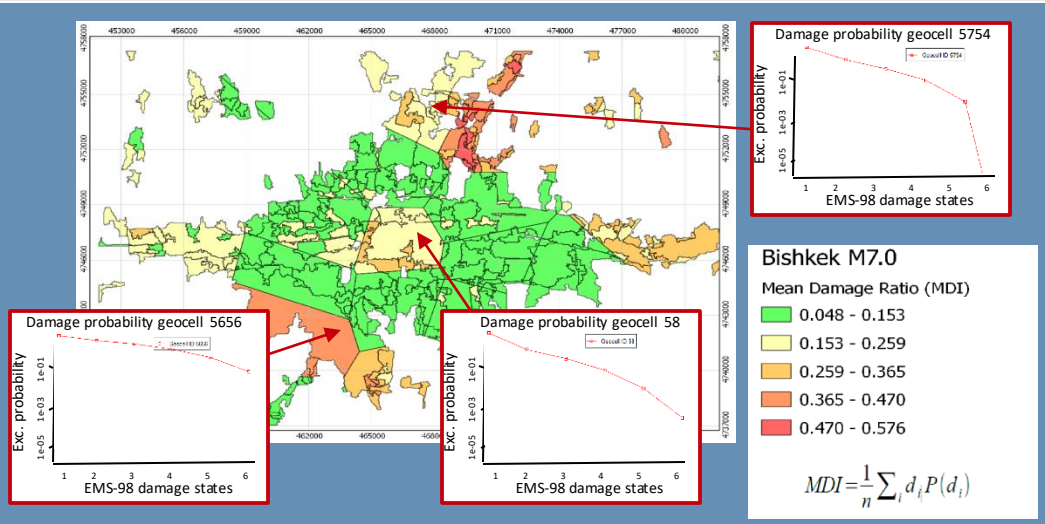

Damage probability of exceedance

Decentralised On Site Early Warning

Low pass filtering

Integration in velocity and displacement

Event detection

(possibility of combining info from the low and high pass filtered record or pred period)

PGV estimation (mean +/- s)

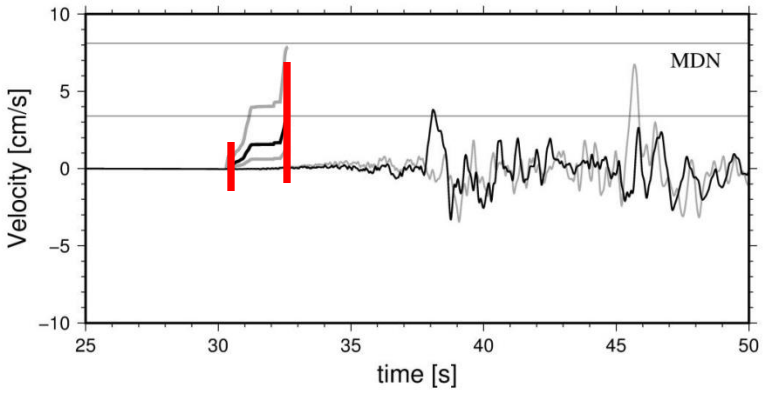

M 5.9 20th May 2012 Emilia earthquake

mean + σ > 8.1 cm/sec Intensity ≥VI

	mean − σ >**8.1** cm/sec	**8.1** cm/sec>mean − σ > **3.4** cm/sec	mean − σ <**3.4** cm/sec
Mean >**8.1** cm/sec			
8.1 cm/sec>mean>**3.4** cm/sec			
Mean <3.4 cm/sec			

8.1 cm/sec > mean + σ > 3.4 cm/sec Intensity =V

	mean − σ >**8.1** cm/sec	**8.1** cm/sec>mean − σ > **3.4** cm/sec	mean − σ <**3.4** cm/sec
Mean >**8.1** cm/sec			
8.1 cm/sec>mean>**3.4** cm/sec			
Mean <**3.4** cm/sec			X

mean + σ < 3.4 cm/sec Intensity ≤IV

	mean − σ >**8.1** cm/sec	**8.1** cm/sec>mean − σ > **3.4** cm/sec	mean − σ <**3.4** cm/sec
Mean >**8.1** cm/sec			
8.1 cm/sec>mean>**3.4** cm/sec			
Mean <**3.4** cm/sec			X

from
Parolai et al.,2015

Decentralised Onsite-Early Warning

GFZ-Sentry Software, based on Parolai et al. (2015) and developed in cooperation with GEMPA GmbH.

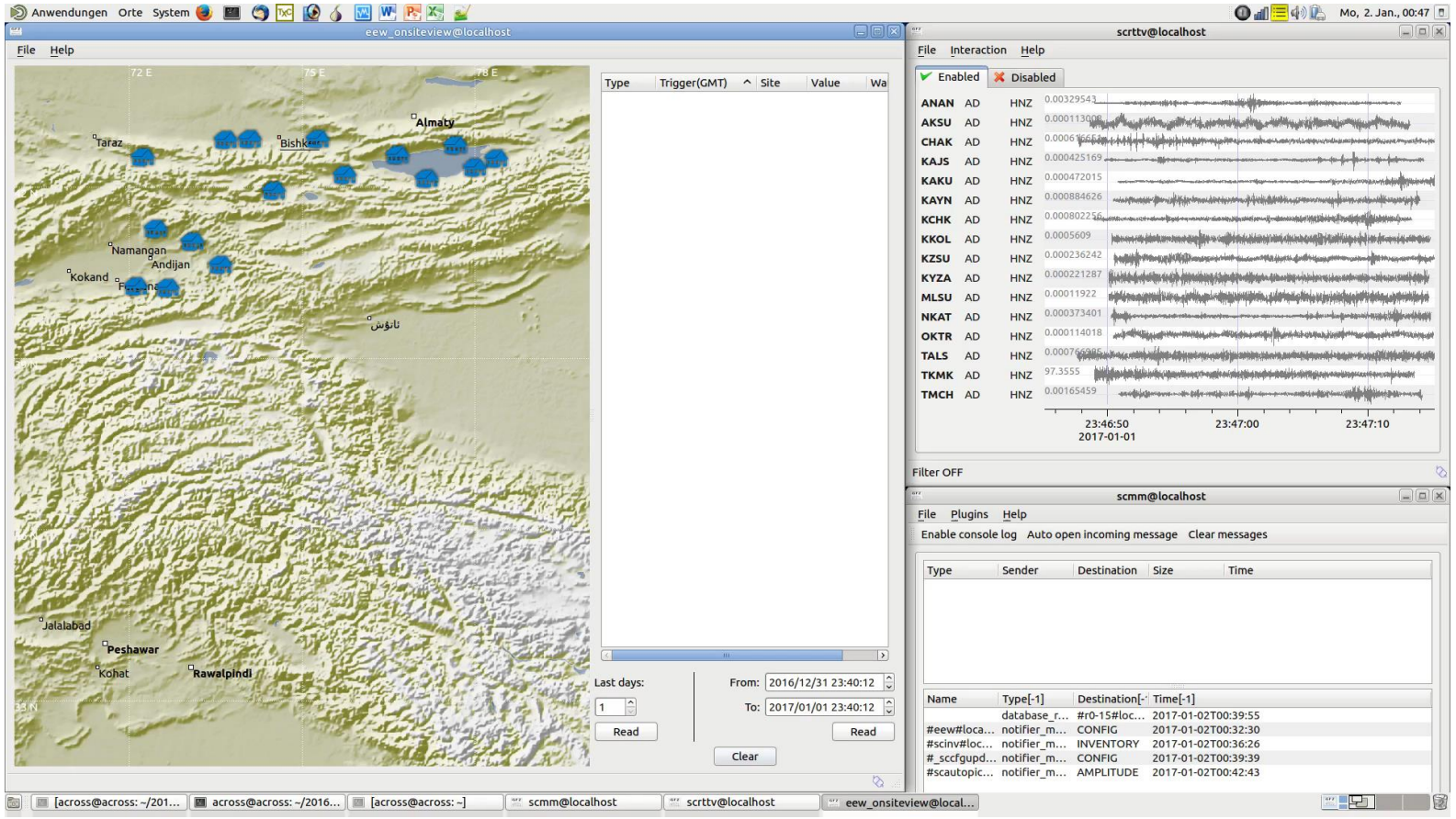

Decentralised OSEW in testing

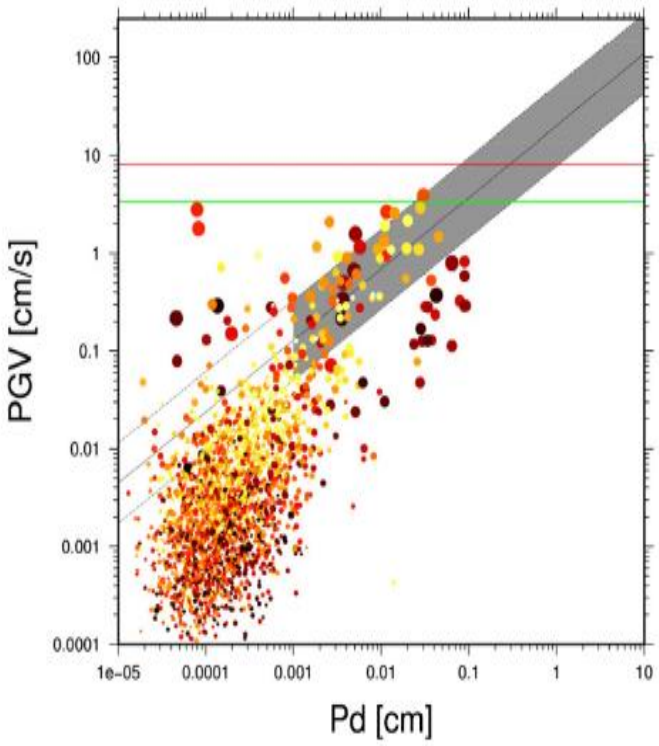

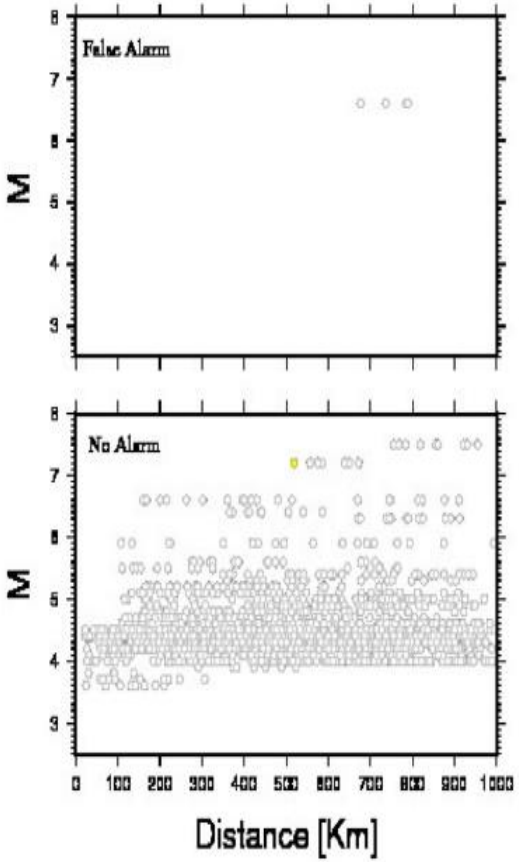

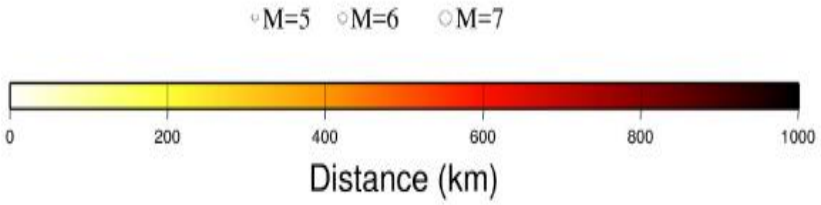

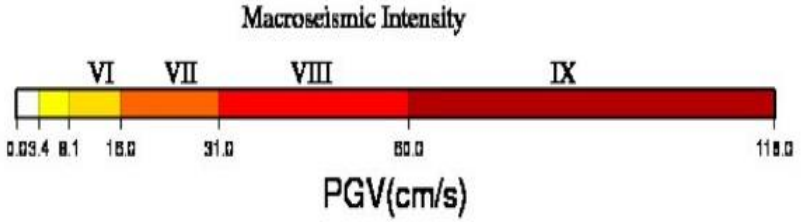

from Parolai et al.,2017, Frontiers

Application to KiK-Net and K-NET recordings

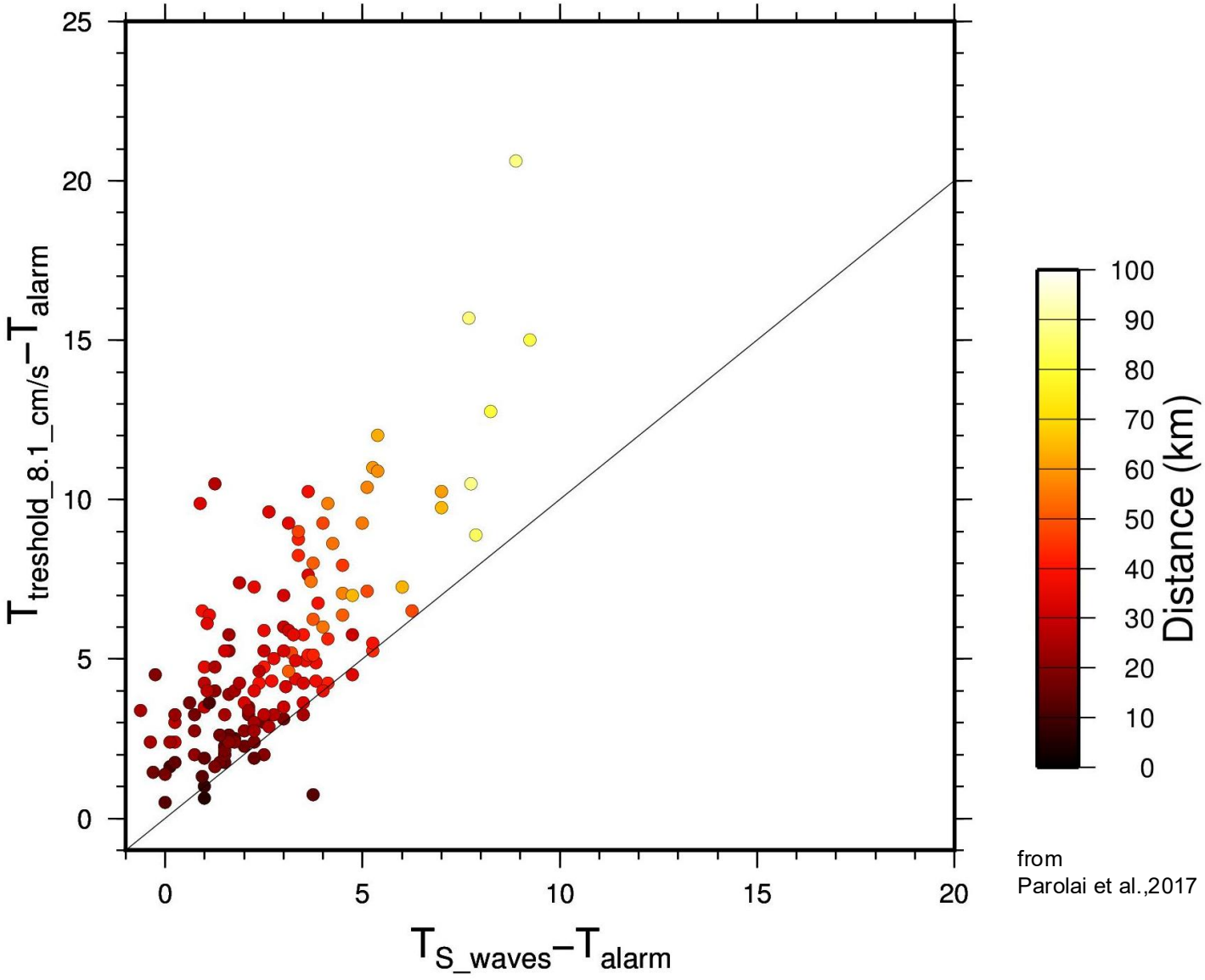

from
Parolai et al.,2017

Offline application to Kyrgyzstan: Lead time for Repetition of the M 7.8 1911 Kemin Earthquake

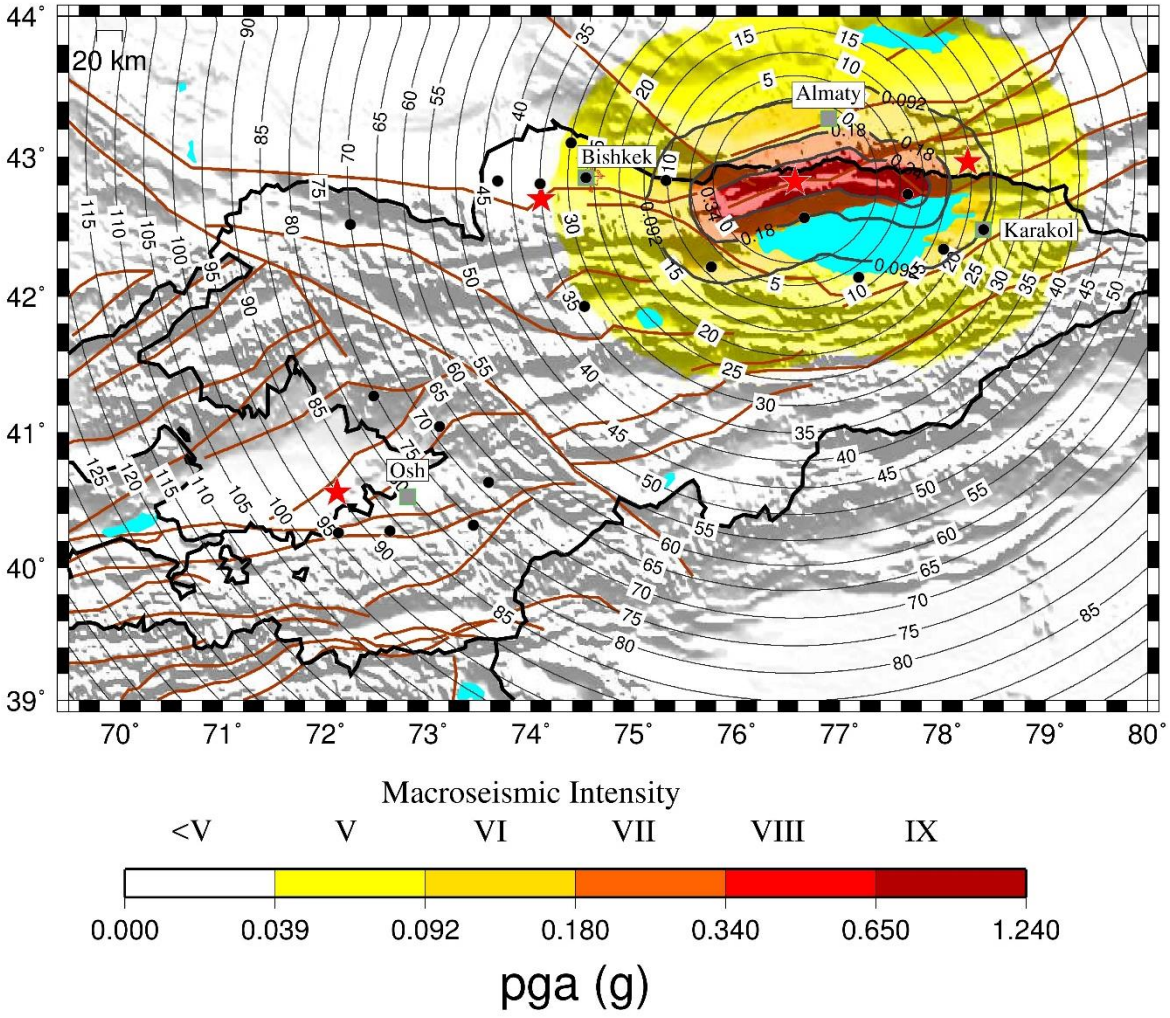

from
Parolai et al.,2017, Frontiers

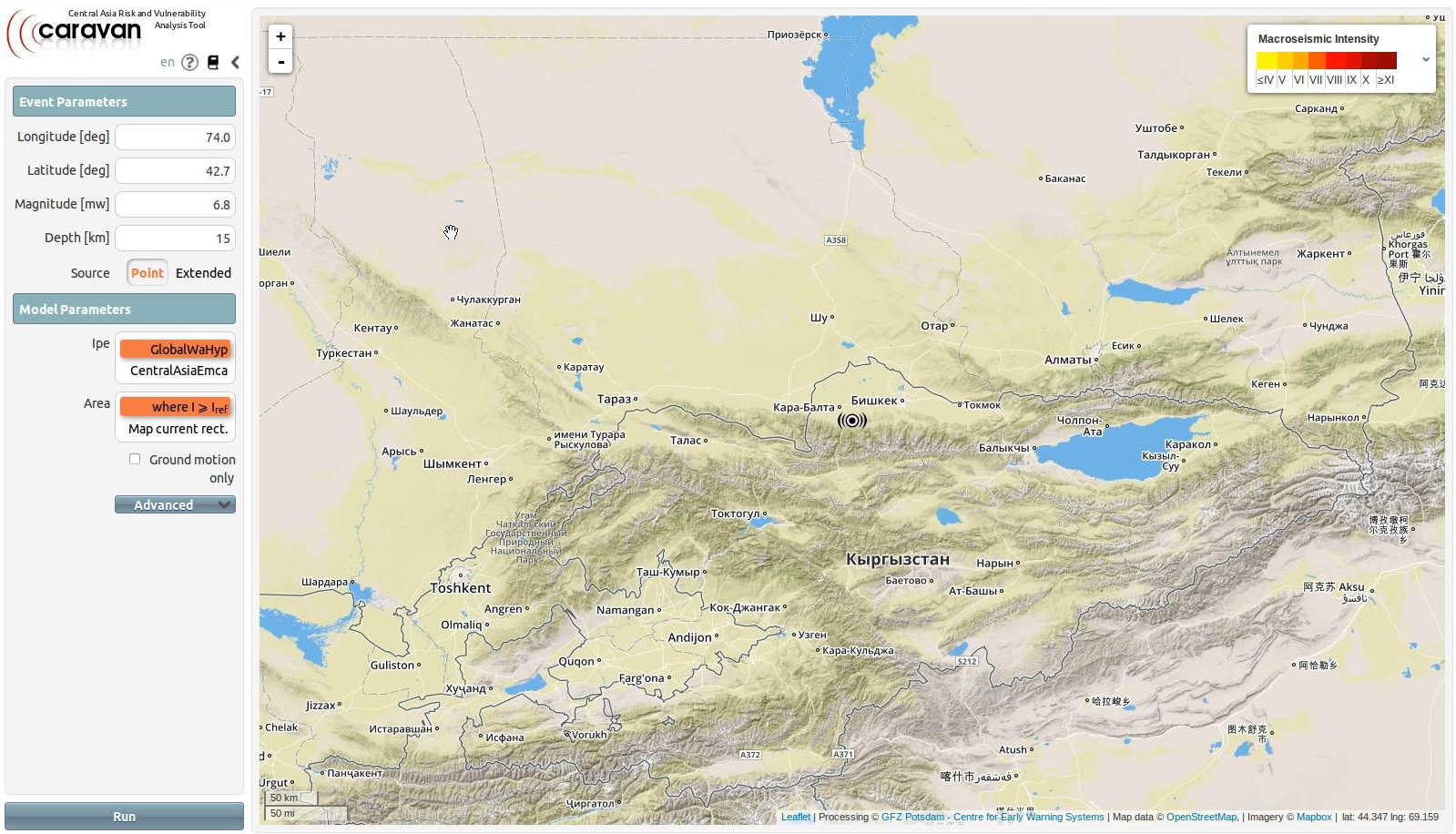
Central Asia Risk and Vulnerability Analysis Tool
caravan
en
Event Parameters
Longitude [deg]
74.0
Latitude [deg]
42.7
Magnitude [mw]
6.8
Depth [km]
15
Source
Point
Extended
Model Parameters
Ipe
GlobalWaHyp
CentralAsiaEmca
Area
where I ⩾ Iref
Map current rect.
Ground motion only
Advanced
Run
Macroseismic Intensity
≤IV V VI VII VIII IX X ≥XI
Приозёрск
Сарканд
Ушгобе
Талдыкорган
Текели
Баканас
Жаркент
Чулаккурган
Кентау
Жанатас
Туркестан
Каратау
Шу
Отар
Шелек
Чунджа
Есик
Алматы
Кеген
Тараз
Бишкек
Токмок
Кара-Балта
Чолпон-Ата
Нарынкол
Каракол
Балыкчы
Кызыл-Суу
Шаульдер
имени Турара Рыскулова
Талас
Арысь
Шымкент
Ленгер
Токтогул
Кыргызстан
Нарын
Баетово
Ат-Башы
Таш-Кумыр
Шардара
Toshkent
Angren
Namangan
Кок-Джангак
Olmaliq
Andijon
Узген
Кара-Кульджа
Guliston
Quqon
Farg'ona
Хужанд
Jizzax
Chelak
Истаравшан
Исфана
Vorukh
Atush
Пенджикент
Чиргатол
Aksu
50 km
50 mi
Leaflet | Processing © GFZ Potsdam - Centre for Early Warning Systems | Map data © OpenStreetMap, | Imagery © Mapbox | lat: 44.347 lng: 69.159

1976 Seismic Sequence

MessaggeroVeneto

Catastrofico terremoto in Friuli

ALLE 21 UNA SCOSSA SISMICA DELL'OTTAVO GRADO DELLA SCALA MERCALLI HA DEVASTATO MAIANO, BUIA, GEMONA, OSOPPO, MAGNANO, ARTEGNA, COLLOREDO, TARCENTO, FORGARIA, VITO D'ASIO E MOLTI ALTRI PAESI DELLA PEDEMONTANA - GENEROSA OPERA DI SOCCORSO PER ESTRARRE LE VITTIME DALLE MACERIE - A UDINE E IN TUTTI I CENTRI DELLA REGIONE UNA NOTTE DI PAURA E DI VEGLIA ALL'APERTO - L'ALBA CI MOSTRA I SEGNI DELL'IMMANE DISASTRO

Origin time: 20:00:13 UTC
epicenter 46° 17' N - 13° 17' E
Depth: 5 - 12 km

Magnitude: 6.0 mb 6.5 Ms 6.4 ML
Epicentral intensity: X MKS

Max PGA recorded: 0,36 g

Felt at distance of : 579 km
Impact Area : 5.700 km^2
Death toll: 989

People needing shelters: 110.000
Damage: 4.500.000 milions (lire in 1976)

Earthquakes recorded since 1977 (>33.000 events)

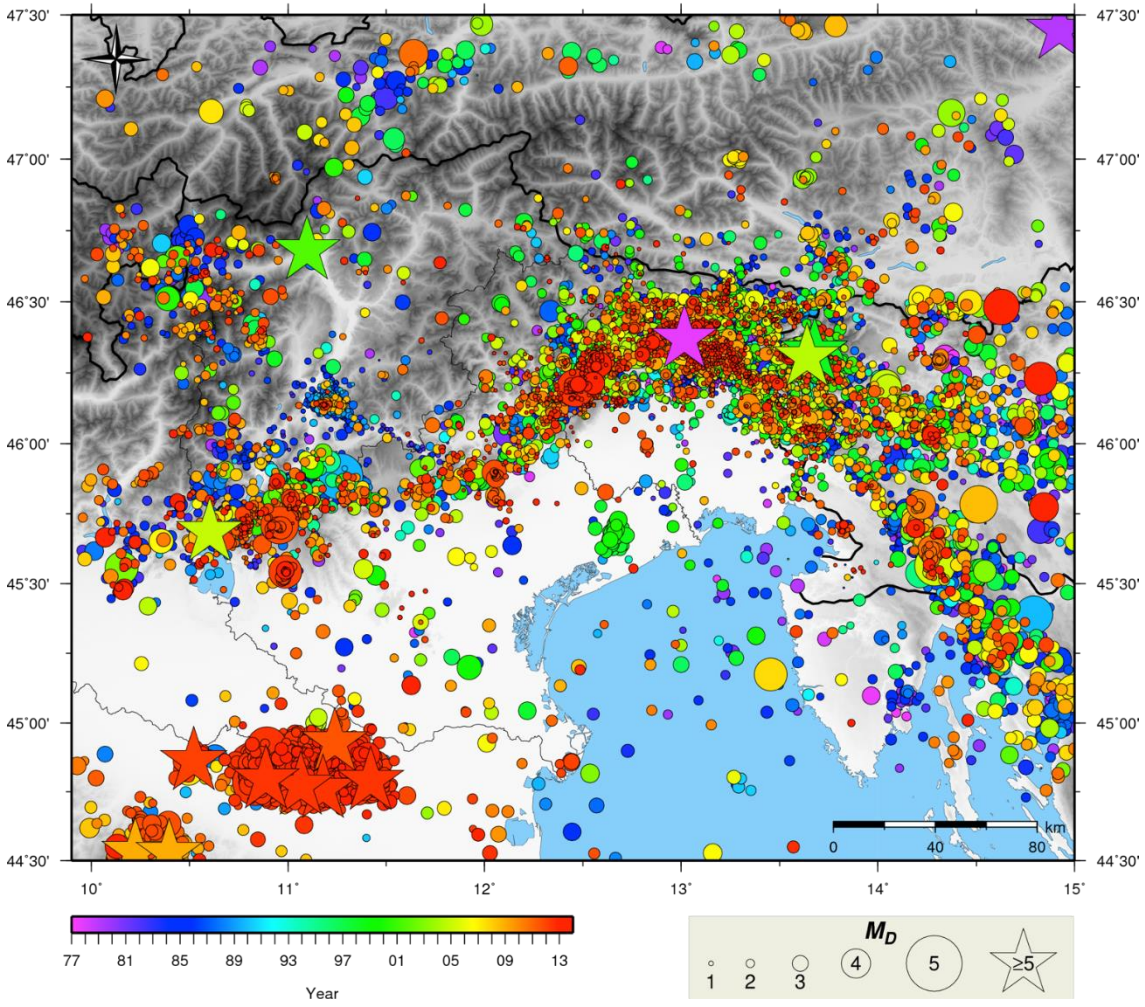

Rapid Damage forecasting in buffer areas

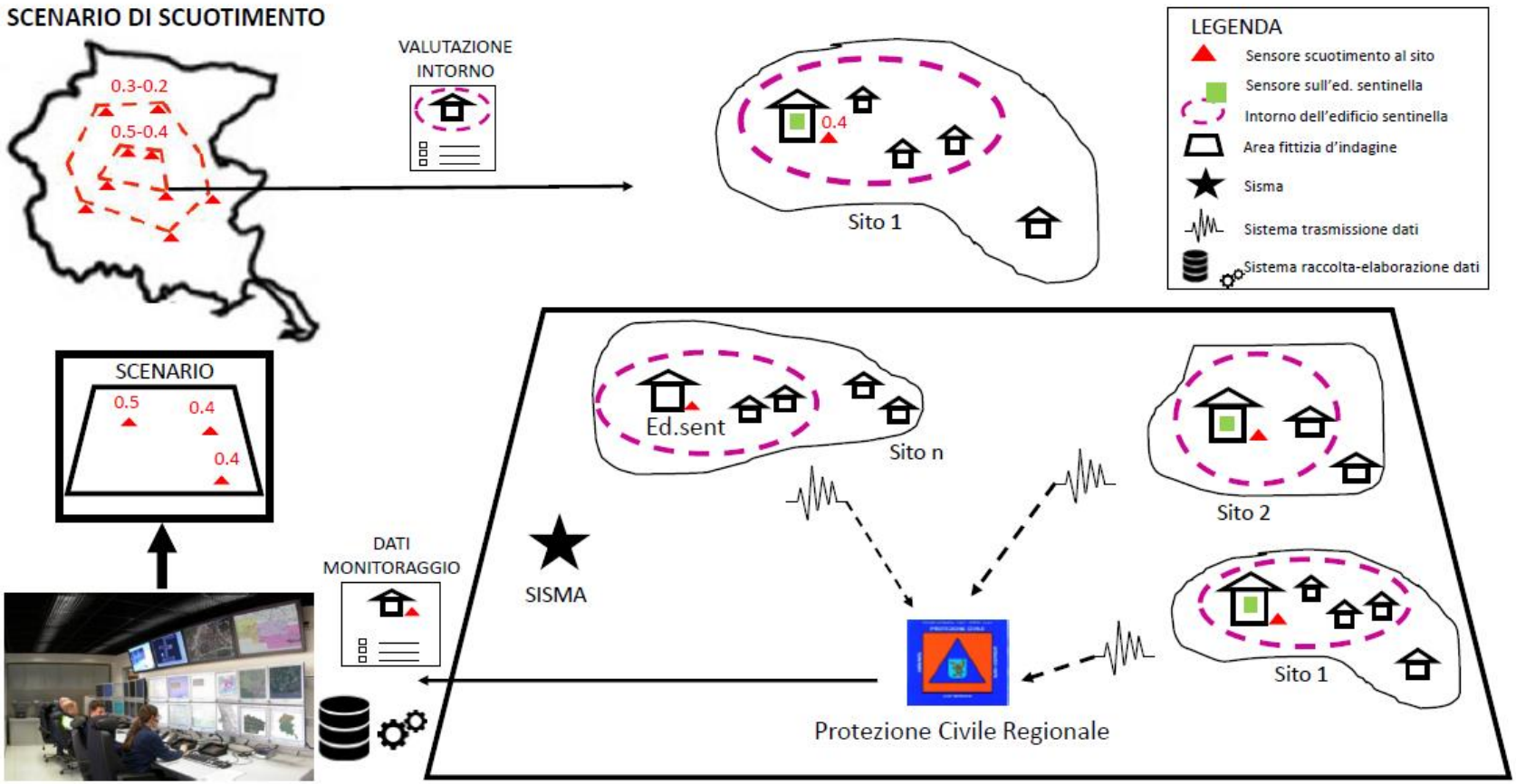

from Grimaz et al.,2017

Method 1

Real time estimation of shaking for different buildings.
Input: base of one of the sentinel building 1) recording at the base of one of the sentinel building (OGS-Uni Trieste)
2) Frequency of oescillation for building type (Uni Udine)

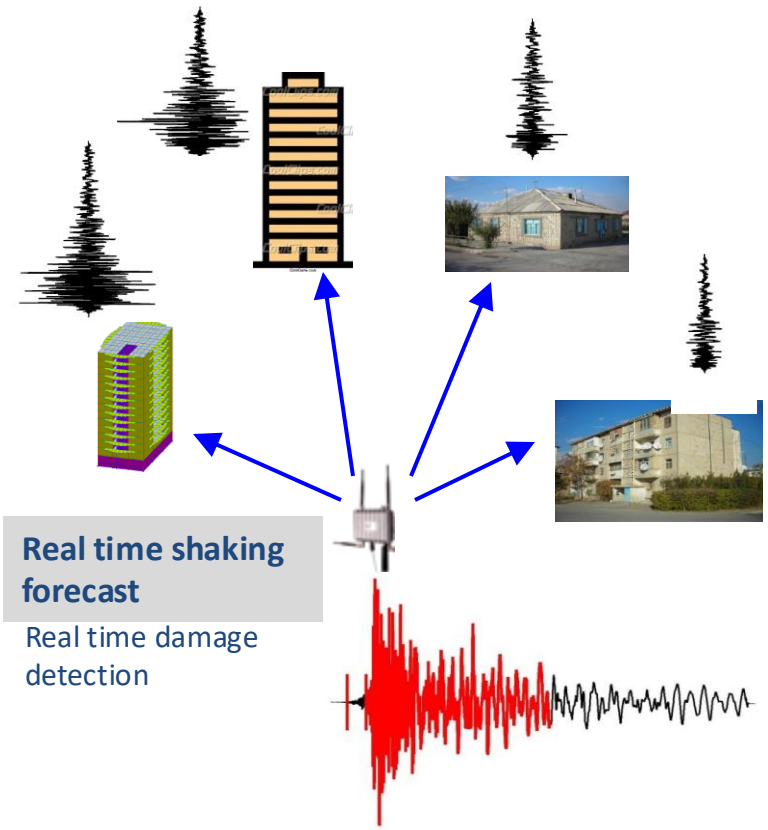

Real time shaking forecast

Real time damage detection

from
Parolai et al.,2015, SRL

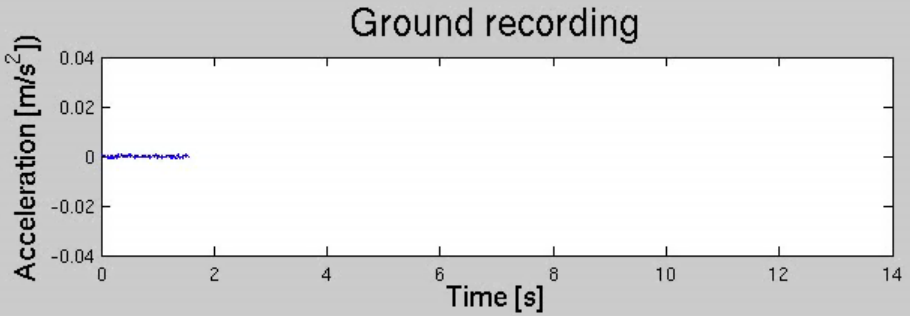

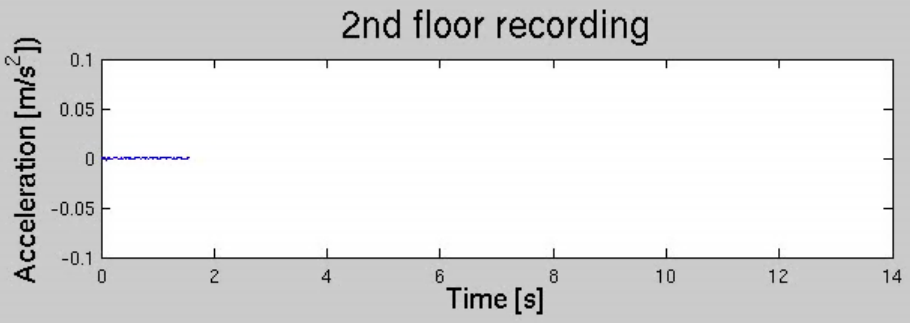

Method 2

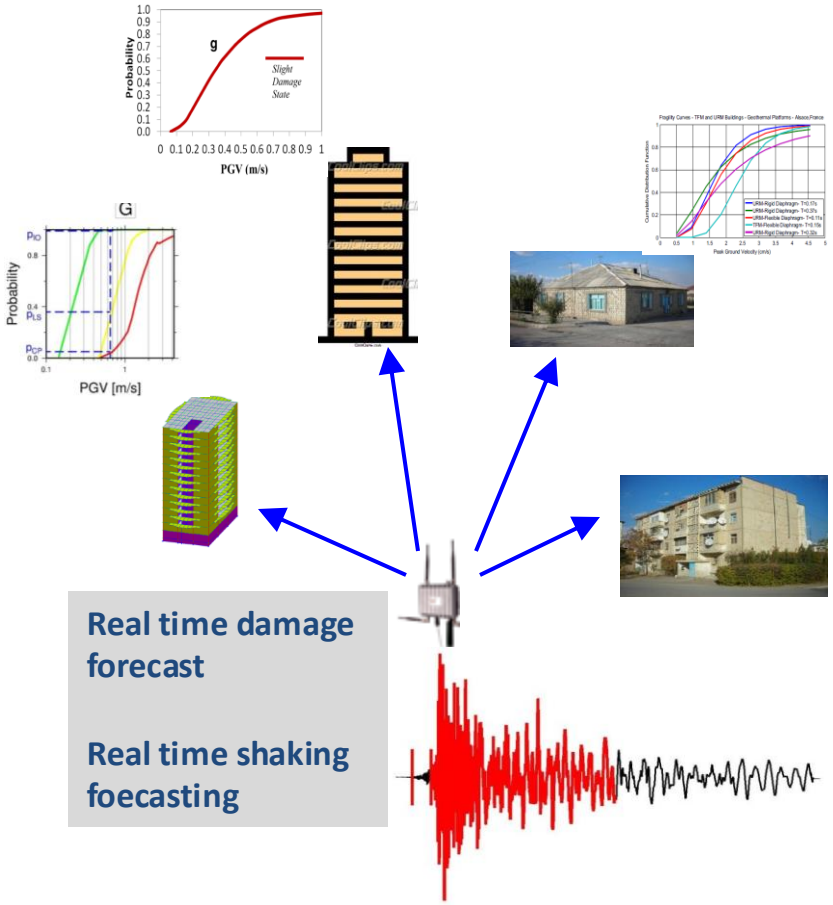

Real time damage forecast

Real time shaking foecasting

from
Parolai et al.,2015, SRL
Megalooikonomou et al. 2018.

Estimation of the probability of exceedance of acertain limit state for different buildings within an area

Input: 1) recording at the base of one of the sentinel building (OGS-Uni Trieste)
2)Fragility curves for building type (Uni Udine)

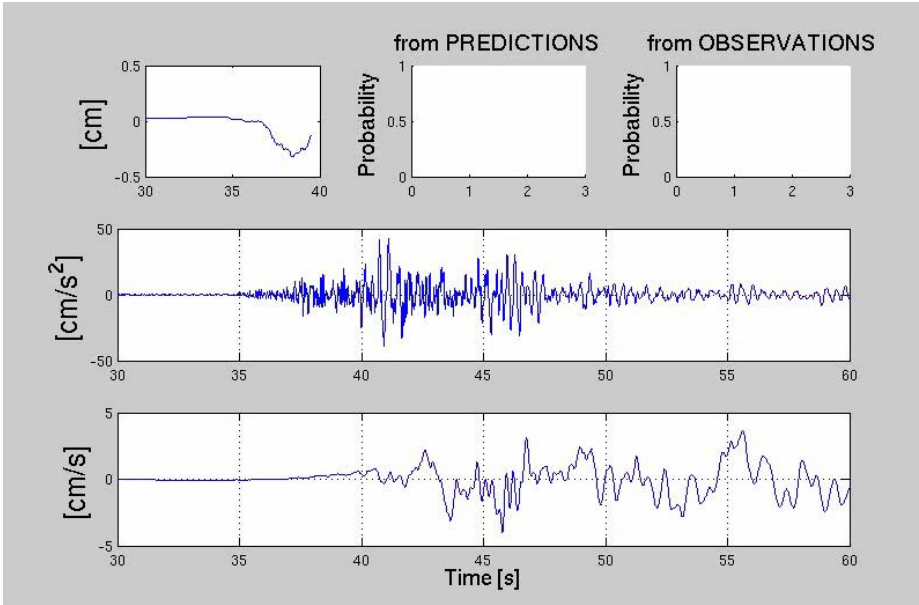

Method 3

First level estimate of possible damage in buildings with sensors at the base and at the top.

Input: 1) recording at the base of one of the sentinel building (OGS-Uni Trieste)

2) Real time measurement of interstorey-drift and/or resonance frequency variation (OGS-Uni Udine)

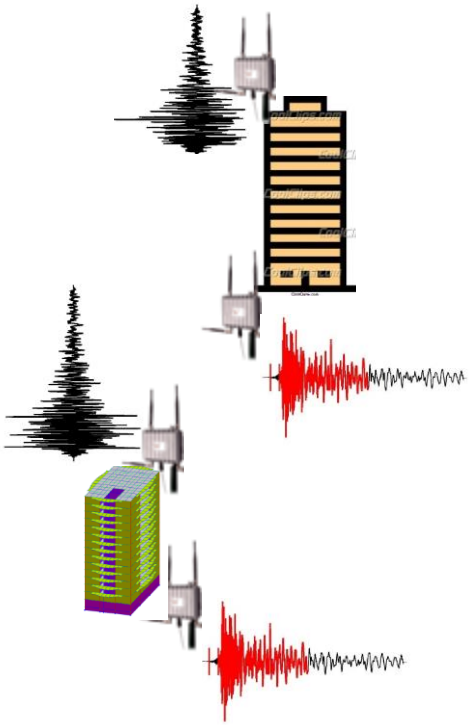

Real time impact forecast

from
Parolai et al.,2015, SRL

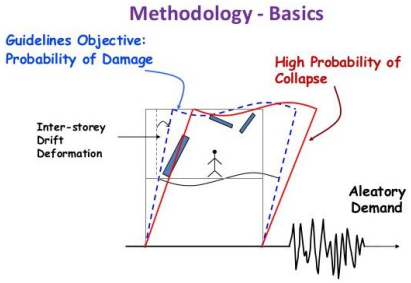

from Pianese et al, 2018

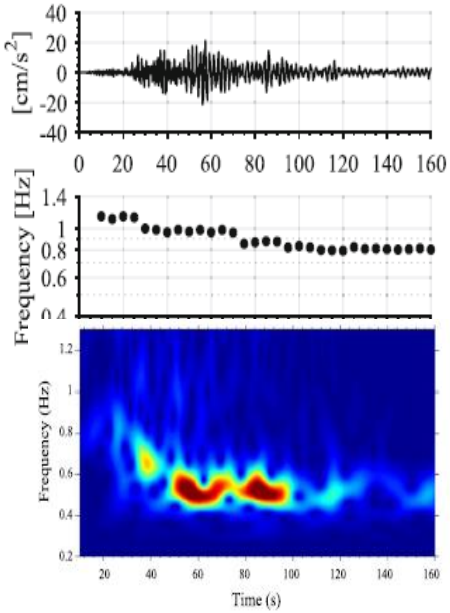

Feasibility for DOSEEW in case of repetition of the 1976 Event

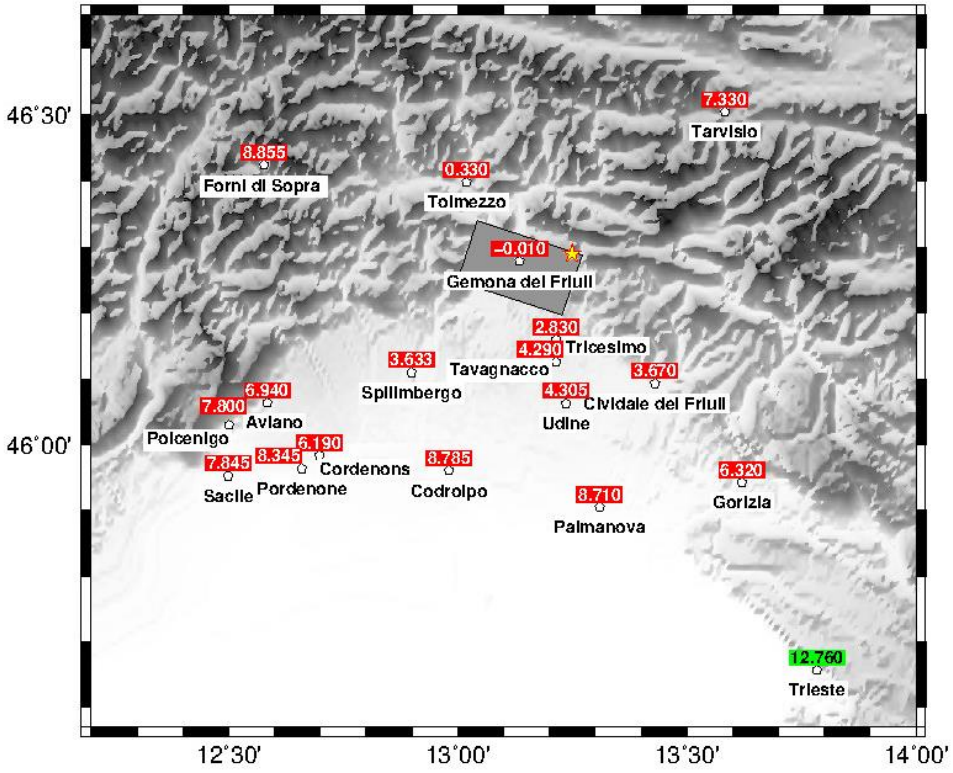

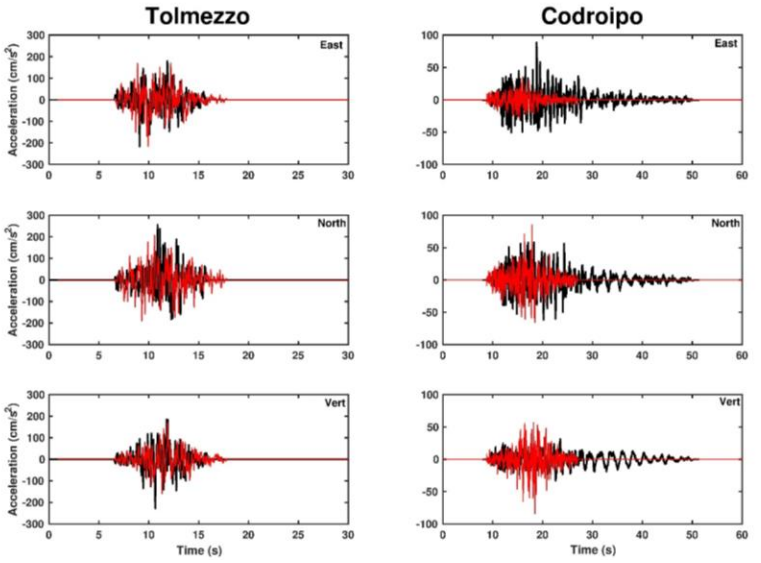

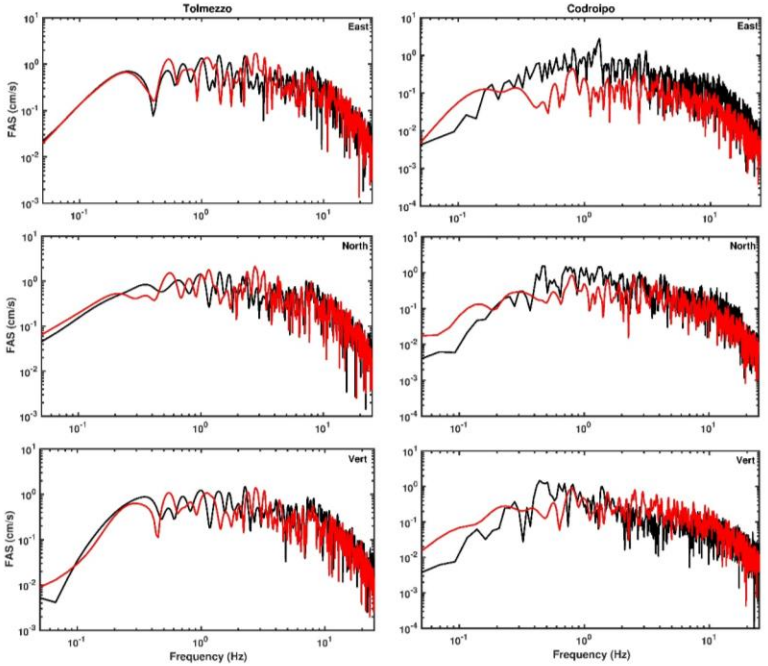

from
Parolai et al.,2020

DOSEEW applied to the synthetic data

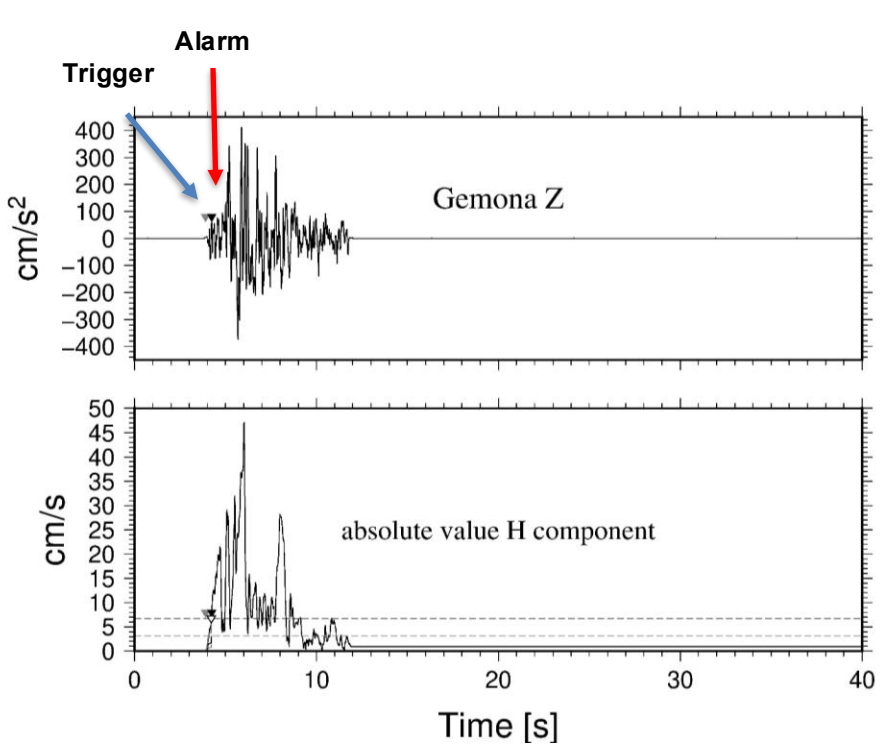

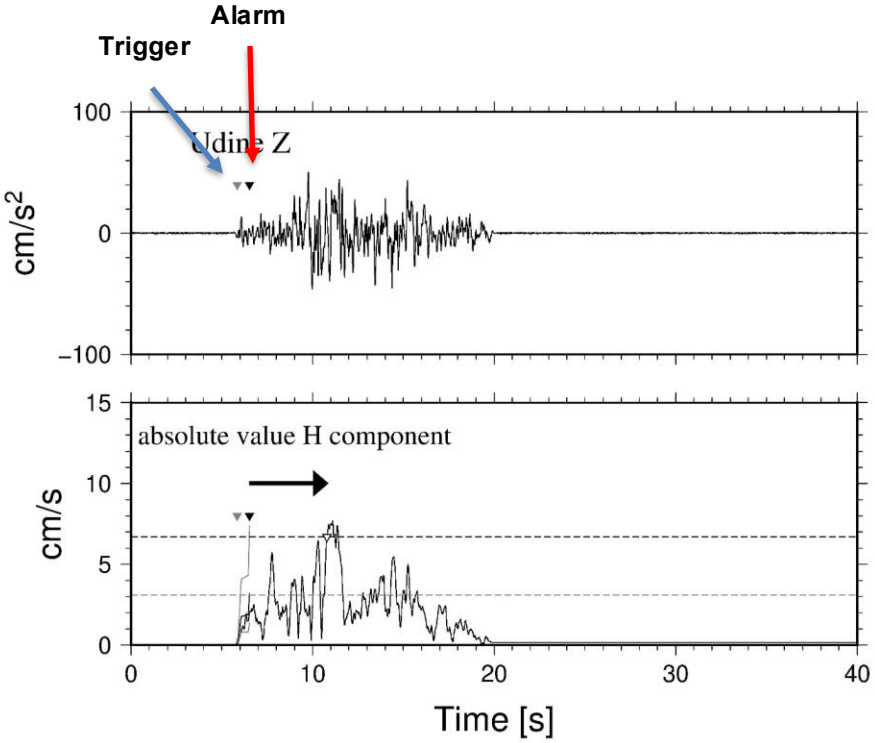

from
Parolai et al.,2020

DOSEEW applied to the synthetic data

Strong dependency of lead-time on slip distribution

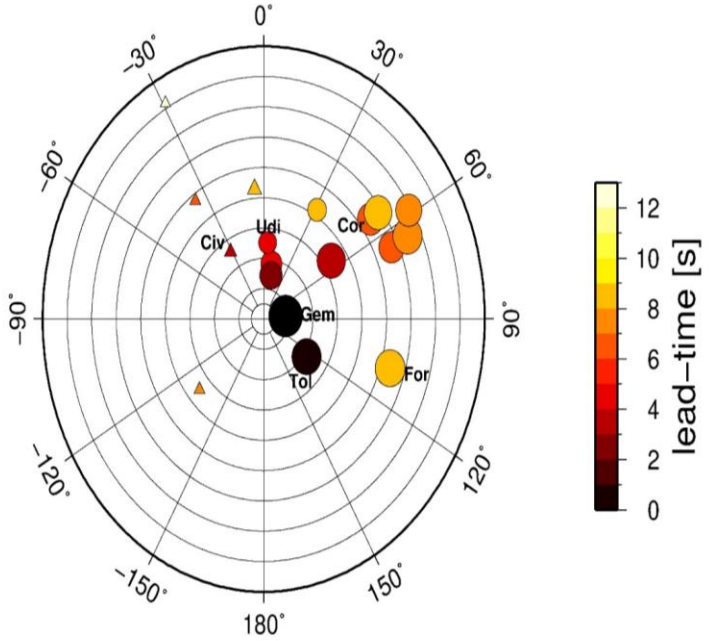

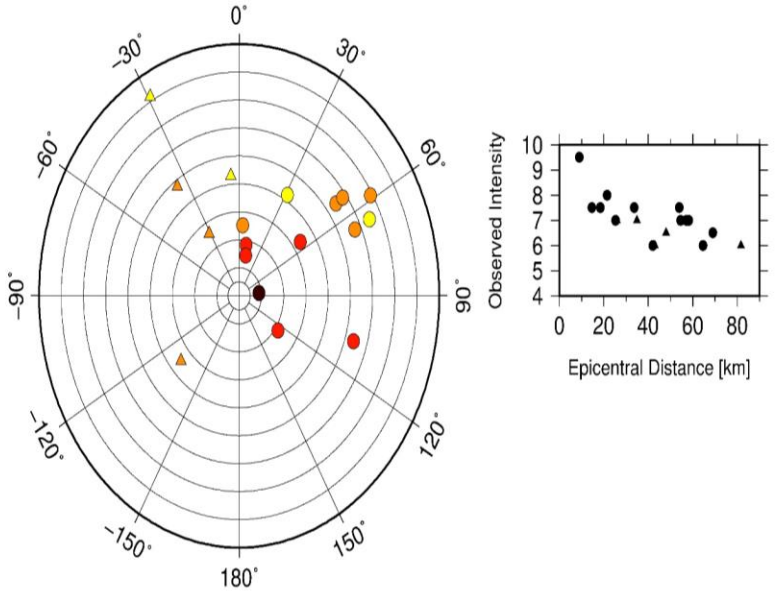

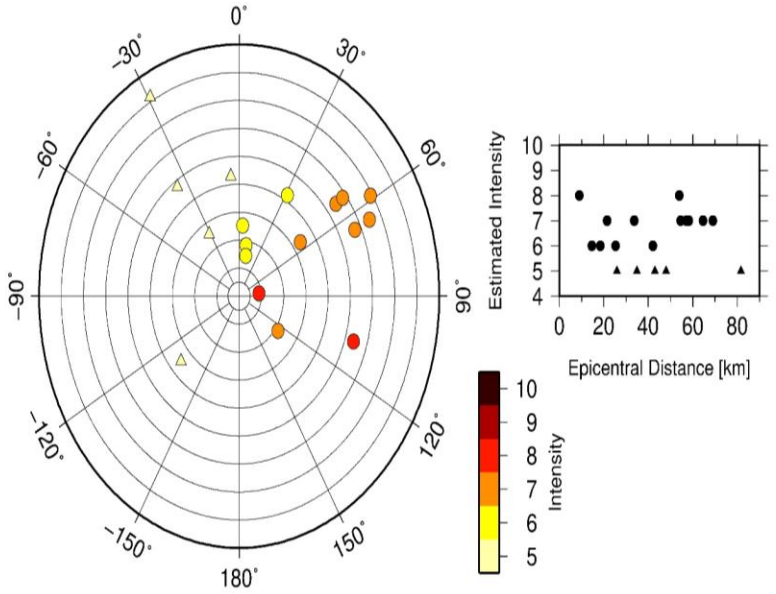

from
Parolai et al.,2020

Possible reduction of 10% of injured persons

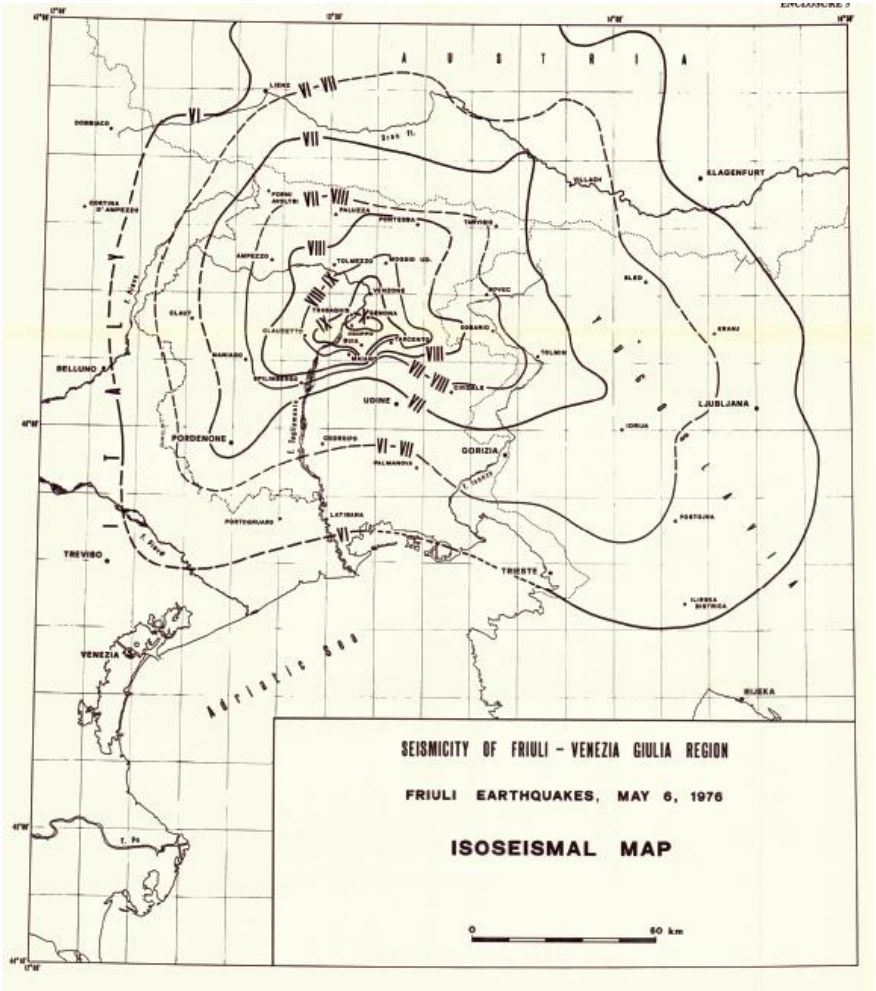

from
Parolai et al.,2020

Table 1 - Summary of the localities and lead times vs injured person during the 1976 Friuli earthquake.

Locality	Lead time (s)	1976 Intensity	1976 Injured
Cividale	3.67	VII	18
Cordenons	6.19	VII	5
Tarvisio	7.33	VII	5
Pordenone	8.34	VII	27
Udine	4.30	VII	53
Forni di Sopra	8.85	VII-VIII	4
Sacile	7.84	VI-VII	6
Tavagnacco	4.29	VII-VIII	24
Spilimbergo	3.63	VII-VIII	10
Tricesimo	2.83	VII-VIII	10

Possible several seconds to stop the plant of TAL

No action was possible for this scenario for the Magnetic Marelli being in the blind zone

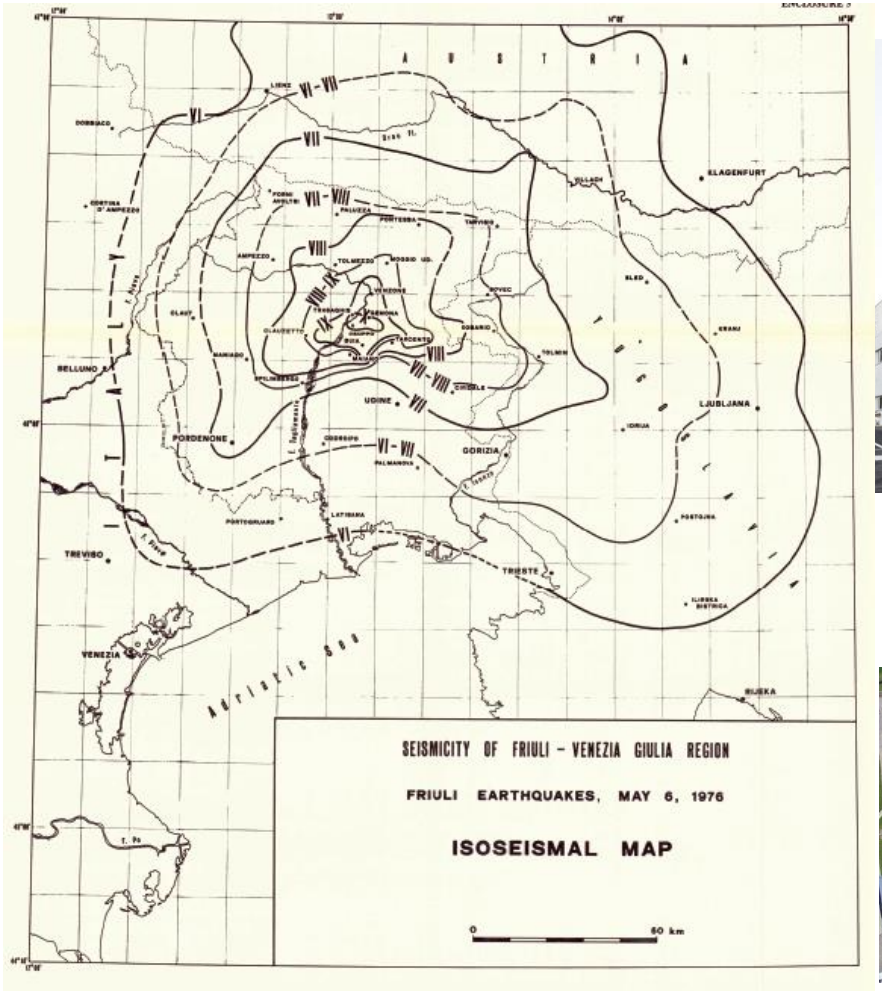

from
Parolai et al.,2020

Magneti Marelli Automotive Lighting, Tolmezzo (UD)

- production of electronic
- components for LED lights
- 5.000 m^2
- > 1100 employees

TAL – Transalpine Pipeline

- Italy, Austria and Germany
- 40% of the energy needs of Germany and the Czech Republic, and 90% of Austria
- 753 km
- 7500 m^3/h
- 750 employees involved
- 1.2 x 10^9 €

Seismic interferometry: soil-structure interaction

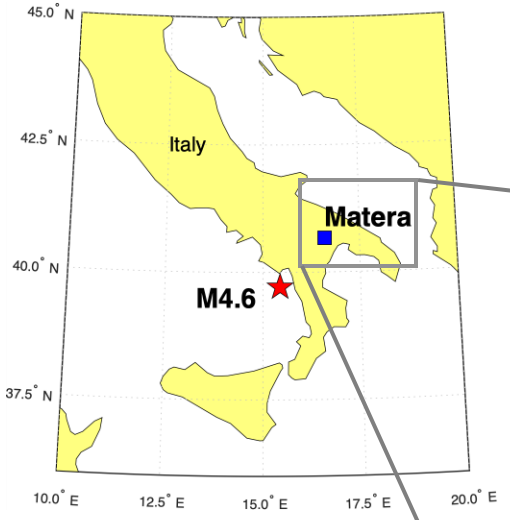

Matera experiment

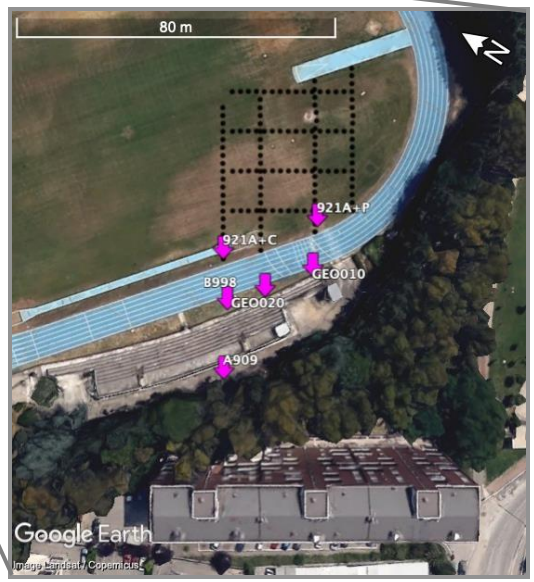

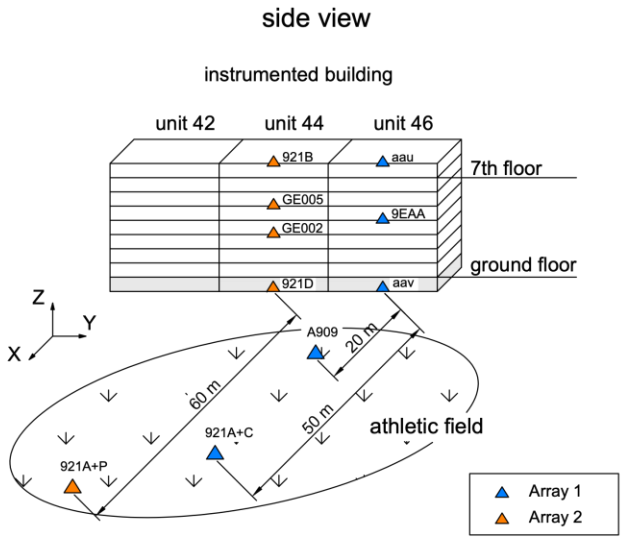

Data recorded on 23-24-25/10/2019

- Seismic noise
- Earthquake: M4.6 event on 25/10/2019

MODERN
Advanced SeisMic InterferOmetry MethoDs and TechnologiEs for EngineeRiNg Seismology

UNIVERSITÀ DEGLI STUDI DI TRIESTE

Seismic interferometry: soil-structure interaction

1. Resonant frequency of the structure

Information on the frequency band of interest

2. Deconvolution

Combined analysis of the recordings from the building and surroundings

3. Phase identification, wavefield reconstruction

Identification of the phases transmitted from the structure

4. Polarization analysis

Identification of different waves and their respective contribution

$$SR_{tb} = \frac{top\ spectra}{bottom\ spectra}$$

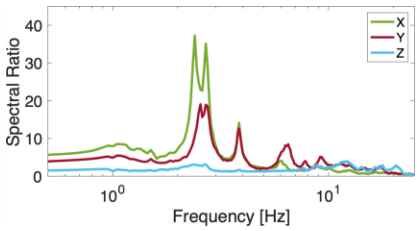

$$S(f) = \frac{u_1(x_1, z_1, f)\, u_2^*(x_2, z_2, f)}{|u_2(x_2, z_2, f)|^2 + \varepsilon}$$

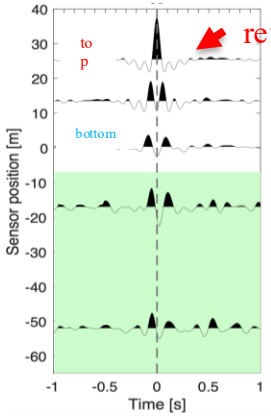

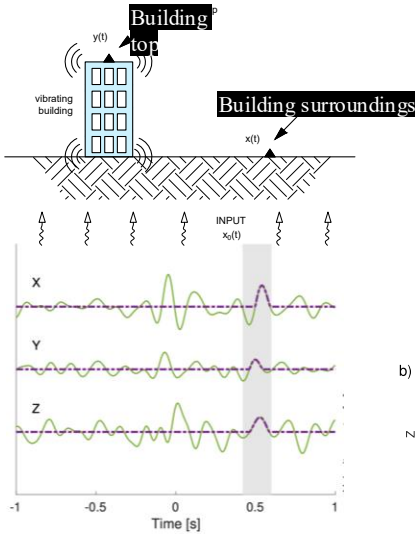

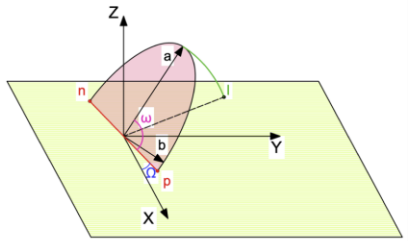

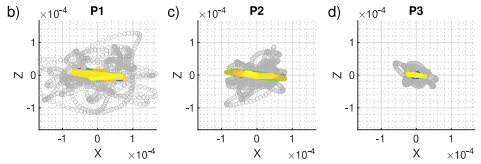

MODERN

Advanced SeisMic InterferOmetry MethoDs and TechnologiEs for EngineeRiNg Seismology

Step 3. Phase identification

Analytical model

- Based on **simplified geometry**
- **Transfer function** between the building and the ground sensors

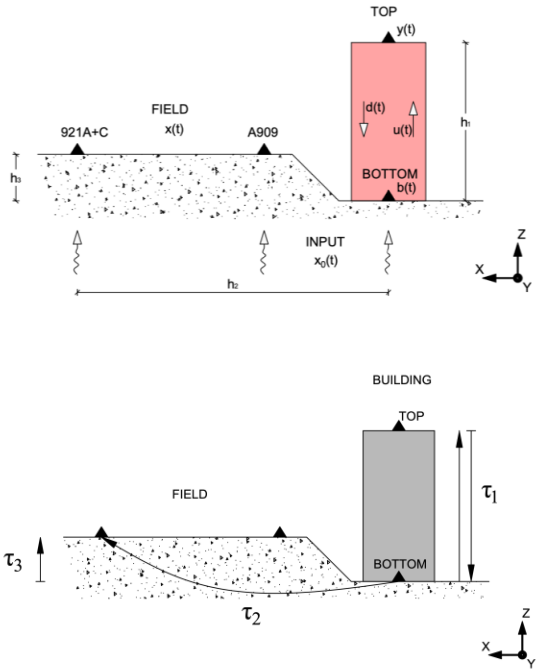

$$\frac{X(f)}{Y(f)} = P_1 + P_2 + P_3$$

$$P_1 = \frac{1}{1+r} e^{-i2\pi f(-\tau_1+\tau_3)},$$

$$P_2 = \frac{r}{1+r} e^{-i2\pi f(\tau_1+\tau_3)},$$

$$P_3 = \frac{(1-r)}{2} e^{-i2\pi f(\tau_1+\tau_2+\tau_3)}.$$

Constrained deconvolution

- Based on the method proposed by Bindi et al. (2010)
- **Phase corresponding to the radiated wavefield**

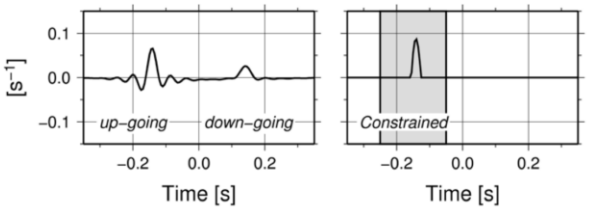

MODERN
Advanced SeisMic InterferOmetry MethoDs and TechnologiEs for EngineeRiNg Seismology

UNIVERSITÀ DEGLI STUDI DI TRIESTE

Matera experiment – results
Phase identification

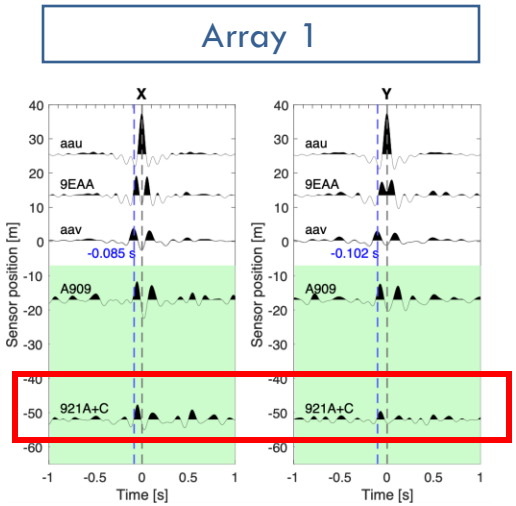

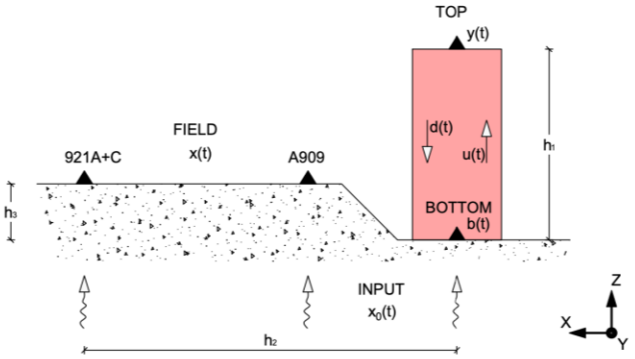

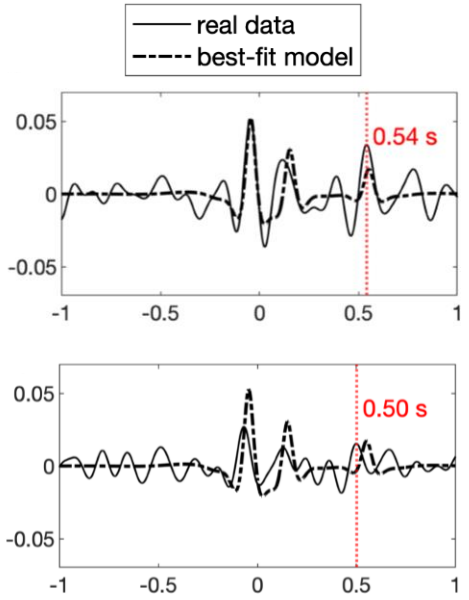

Assumptions for the model:

- Input -> vertically propagating plane wave
- Simplified geometry
- The transfer function between the field sensors and the reference sensor at the top of the building

- Frequency band 2-10 Hz
- Searched parameters – time delays of the wave propagation in the building and the soil

MODERN
Advanced SeisMic InterferOmetry MethoDs and TechnologiEs for EngineeRiNg Seismology

UNIVERSITÀ DEGLI STUDI DI TRIESTE

Seismic interferometry: soil-structure interaction

- The proposed approach allows the **wave-field related to the energy radiated from a vibrating structure** to its surroundings on the surface to be separate and to identify **the wave types.**
- In the Matera experiment, the most significant impact of the vibrating building on the ground motion is **near the resonant frequencies of the building and it is due to quasi Rayleigh or quasi Love waves**
- The knowledge of the dominant wavelength of the radiated wavefield, combined with the polarization analysis => information **about locations of positive and negative wavefield interference** for a given earthquake motion